

## A simple model for simulation of insect pheromone dispersion within forest canopies

Tara Strand<sup>a,b,\*</sup>, Brian Lamb<sup>a,1</sup>, Harold Thistle<sup>c,2</sup>, Eugene Allwine<sup>a,1</sup>, Holly Peterson<sup>d,3</sup>

<sup>a</sup> Laboratory for Atmospheric Research, Department of Civil and Environmental Engineering, Washington State University, Pullman, WA 99164-2910, United States

<sup>b</sup> AIRFIRE Team, Pacific Wildland Fire Sciences Laboratory, U.S.D.A. Forest Service, 400 N 34th St. suite 201, Seattle, WA 98103, United States

<sup>c</sup> U.S.D.A. Forest Service, FHTET, 180 Canfield St., Morgantown, WV 26505, United States

<sup>d</sup> Department of Environmental Engineering, Montana Technical University, 1300 West Park, Butte, MT 59701, United States

### ARTICLE INFO

#### Article history:

Received 12 June 2006

Received in revised form 17 October 2008

Accepted 25 November 2008

Available online 21 January 2009

#### Keywords:

In-canopy dispersion

Bark beetle

Instantaneous

Lagrangian

Tracer

### ABSTRACT

Synthetic pheromones and other behavioral chemicals are used by land managers to prevent insect-caused tree mortality or crop failure in forest and agricultural systems. Currently, no method exists to continuously measure pheromone concentration or movement in real-time. To improve our understanding of pheromone fate and transport under different forest canopies, results from a set of surrogate pheromone (sulfur hexafluoride tracer) experimental trials were used to evaluate a simple, instantaneous, three-dimensional Lagrangian dispersion model. The model was designed to predict both instantaneous and time-averaged pheromone concentrations. Overall, the results from the model show simulated time-averaged arc maximum concentrations within a factor of two of the observed data. The model correctly matched the sharp peaks and narrow widths of the meandering plumes observed in the instantaneous data, however the magnitude of the instantaneous peaks was often under-estimated. This model and evaluation provide the basis for a tool that can be used to guide deployment of synthetic pheromones or other semiochemicals for monitoring, mass trapping, or disruption of mating or aggregation.

Published by Elsevier B.V.

### 1. Introduction

Foresters and land managers use synthetic pheromones to monitor populations, to mass trap, and to deter destructive outbreaks of insects by disrupting aggregation or mating. Two major groups of forest insect pests are conifer-feeding bark beetles (Seybold et al., 2000) and forest-defoliating moths (Furniss and Carolin, 1977). Results from bark beetle pest control strategies utilizing synthetic pheromone deployment have shown unpredictability in preventing mass attacks (Shea et al., 1992; Borden, 1995; Holsten et al., 2002). This inconsistency could be due to a lack of information regarding insect response patterns; to problems with the pheromone release devices themselves; or to a lack of understanding of pheromone plume dispersion within forest canopies (Holsten et al., 2003). In particular, the influence of forest micrometeorology and turbulence on pheromone plume spread and transport has not been well documented (Fares et al., 1980).

Direct measurement of pheromone concentrations in ambient air is extremely difficult, and no robust continuous fast response instrument exists for measurement of instantaneous pheromone concentrations. Electroantennographic (EAG) recording with live insect antennae can be used to detect the presence of pheromones in a forest canopy in terms of relative units (Färbert et al., 1997); however, in situ readings from the EAG may represent all stimuli the antenna is experiencing, not just those from the pheromone plume of interest (Murlis et al., 2000). Recently, a calibration system was developed to convert relative units to absolute units by using the sex pheromone for the pink bollworm moth, *Pectinophora gossypiella* (Saunders) (Koch et al., 2002). To the authors' knowledge, this approach has yet to be used to directly measure pheromone in absolute units or to characterize pheromone plume transport and dispersion in forests.

Despite the early stages of in situ pheromone concentration measurement, temporal and spatial characteristics of pheromone plumes have been characterized through tracer studies (Murlis and Jones, 1981; Murlis et al., 2000; Thistle et al., 2004) and insect flight behavior studies (Aylor, 1976; Elkinton et al., 1984; Salom and McLean, 1991). A tracer is an easy to measure substance (mass or electrically charged ion field) that is used to characterize and quantify fluid motion and/or movement of mass due to fluid flow. A tracer is usually employed as a surrogate for a mass that is difficult to measure in situ. Results from surrogate pheromone (tracer) field

\* Corresponding author. Tel.: +1 206 732 7867; fax: +1 206 732 7801.

E-mail addresses: [tarastrand@fs.fed.us](mailto:tarastrand@fs.fed.us) (T. Strand), [blamb@wsu.edu](mailto:blamb@wsu.edu) (B. Lamb), [hthistle@fs.fed.us](mailto:hthistle@fs.fed.us) (H. Thistle), [allwine@mail.wsu.edu](mailto:allwine@mail.wsu.edu), [hpeter@mttech.edu](mailto:hpeter@mttech.edu) (H. Peterson).

<sup>1</sup> Tel.: +1 509 335 2576; fax: +1 509 335 7632.

<sup>2</sup> Tel.: +1 304 285 1574.

<sup>3</sup> Tel.: +1 406 496 4339.

studies conceptually describe pheromone concentration fields in terms of thin filaments of plume that meander in a very intermittent manner (Murlis et al., 2000; Thistle et al., 2004). The concentration intermittency – bursts of concentration followed by gaps of no concentration – inside the plume result in concentration fluctuations at a static point downwind or along a trajectory, such as when an insect tracks an odor upwind (Farrell et al., 2002). It is understood that insects respond to instantaneous and peak concentration fields (Aylor, 1976).

Bark beetles and moths respond to pheromone concentration fluctuations on a timescale that is on the order of seconds or smaller. For example, in wind tunnel experiments, Elkinton et al. (1984) found that gypsy moths responded to pheromone odor plumes when time-averaged Gaussian models predicted concentrations to be too low to elicit a gypsy moth response and proposed that this indicated an insect response to concentration fluctuations rather than to the mean concentration. Insect behavior may change in response to the rapidly changing pheromone concentrations within the plume (Murlis and Jones, 1981; Vickers and Baker, 1992; Mafrano and Cardé, 1994) and a mean concentration value measured in minutes, may not reflect the concentration fluctuations influencing insect behavior. Instantaneous concentrations, on the order of seconds or less, should be included in simulated or observed pheromone plume structure analysis.

Pending advancement in instrumentation designed to measure instantaneous pheromone concentration fluctuations, a tracer can be used as a surrogate pheromone to study plume structure on a fine temporal scale. Tracer technology and the use of a tracer to study concentration fluctuations within a plume is well documented (Mylne et al., 1996). Peterson and colleagues (Peterson et al., 1990, 1999; Thistle et al., 2004) have employed sulfur hexafluoride ( $\text{SF}_6$ ) tracer methods to measure instantaneous plume behavior in grassland and forest ecosystems under a variety of meteorological conditions and over distances from a few meters to a few hundred meters. These results clearly show very narrow instantaneous plumes that meander in filaments, have sharp edges, and extremely high peak to mean ratios. These results are not unique, similar findings have been reported from experimental trials conducted in wind tunnels and in the field, using different tracer technologies (Hanna, 1984; Dinar et al., 1988; Lewis and Chatwin, 1995; Mylne et al., 1996; Murlis et al., 2000).

The thin filaments observed during tracer studies are unique when compared to time-averaged plume spread, which can usually be described as cone shaped and moving along the mean wind direction. The filaments can be pictured as thin ribbons extending from the tracer source, and during low wind speed conditions, it is typical for these plumes to meander  $360^\circ$  around the source in a relatively short time span (Thistle et al., 2004). As a result, the downwind concentration field is quickly changing as the filaments expand and move according to the three-dimensional winds.

Models designed to simulate mean concentration fields are inadequate for simulating the filament type plumes observed in the field and are unable to yield instantaneous pheromone concentration fluctuations on a temporal scale known to influence insect behavior (Aylor, 1976). To simulate instantaneous concentration fields both the meandering and the fluctuating temporal scales need to be considered (Hanna, 1986). Models developed to include algorithms for plume meander and internal fluctuation components range in computational intensity from meandering plume models to second order closure models. Sykes and Gabruk (1997) employed a second-order turbulence closure model to calculate instantaneous dispersion downwind from a source. To simulate filament plume meander and internal concentration fluctuations Yee and Wilson (2000) developed a statistical-based algorithm derived from observations of plume behavior in a water channel system. A filament-based, first-order closure model was designed by Farrell

et al. (2002) specifically to simulate odor plumes. These models are computationally intense when compared to those based on the meandering plume theory. The meandering plume model developed by Gifford (1959) simulates plume meander due to eddies larger than the plume, knowledge of the probability density function of the wind field is required beforehand and the model does not simulate in-plume concentration fluctuations owing to eddies smaller than the plume (Reynolds, 2000a). To examine internal concentration fluctuations and plume dispersion, Reynolds (2000a) combined the Gifford (1959) meandering plume model with a Lagrangian stochastic particle model. Peterson et al. (1990) used the meandering plume model theory to develop a model that required no prior knowledge of the wind field to simulate instantaneous fluctuations at a high frequency.

To improve our understanding and ability to simulate pheromone plume transport and dispersion within a forest and to characterize pheromone plume structure in the near field ( $\leq 30$  m), the tracer,  $\text{SF}_6$ , was used as a surrogate pheromone. Two tracer field campaigns were carried out under different coniferous canopy types; lodgepole pine, *Pinus contorta latifolia* (Engelmann) Critchfield, near Potomac, Montana, conducted in July 2000; and ponderosa pine, *Pinus ponderosa* Laws., near LaPine, Oregon, conducted in June 2001. A companion paper, Thistle et al. (2004), describes and presents the results from these field campaigns, including time-averaged and instantaneous surrogate pheromone concentrations, stability conditions, and meteorological parameters. In this paper, we employ these results and the surrogate pheromone data collected in the field to evaluate a simple dispersion model designed to describe instantaneous and time-averaged pheromone plume behavior beneath a forest canopy.

In order to predict pheromone plume concentrations at a frequency that has been shown to elicit a response from an insect, a model that simulates concentration fluctuations on a fine time scale is essential. In this paper, we directly address this need and describe a basic Lagrangian three-dimensional instantaneous dispersion model. The model was modified from the meandering plume model (Peterson et al., 1990; Peterson and Lamb, 1995) to simulate both high-frequency instantaneous puff growth and plume meander. The model uses the Gaussian puff equation to simulate high-frequency (1 Hz) pheromone plume transport and dispersion within forest canopies. As a first step in evaluating the model, surrogate pheromone data from the lodgepole and ponderosa pine experimental trials were used to examine model performance of instantaneous and mean plume behavior. We anticipate that the instantaneous puff dispersion model can be used as a tool to develop guidelines and/or assist land managers in deployment of synthetic pheromones in forests or agricultural stands.

## 2. Description of the experimental trials

Two surrogate pheromone studies were carried out to investigate plume characteristics in the near field ( $\leq 30$  m) under different canopy cover. A companion paper (Thistle et al., 2004) provides additional details on the experimental methods.

### 2.1. Canopy characteristics

The experimental trials were conducted in lodgepole pine (July, 2000, Potomac, Montana) and ponderosa pine (July, 2001, LaPine, Oregon) forests. Density of tree stems (greater than 7.6 cm at dbh) and extent of underbrush were notable differences between the two sites (Table 1; Thistle et al., 2004). Stem density in the lodgepole pine forest (1521 stems/ha) was considerably higher than in the ponderosa pine forest (389 stems/ha). The lodgepole pine canopy was uniform with very little underbrush growing beneath it. Large

**Table 1**  
Canopy metrics<sup>a</sup> of two forest research sites in fairly flat terrain in Montana and Oregon used for the study of pheromone dispersion.

Site	Month–year study conducted	Canopy type	Stems per hectare <sup>b</sup>	Average canopy height (m)	Canopy characteristics	Underbrush characteristics
Potomac, MT	July 2000	Lodgepole pine	1521	30	Uniform	Little to none
LaPine, OR	June 2001	Ponderosa pine	389	35	Large gaps	<i>Ceanothus velutinus</i> <sup>c</sup>

<sup>a</sup> As described by Thistle et al. (2004).

<sup>b</sup> Stems greater than 7.6 cm dbh.

<sup>c</sup> Tallest within the experimental trial was 1.5 m.

gaps in the ponderosa pine canopy were irregular and frequent and the primary understory plant *Ceanothus velutinus*, commonly occurred in the canopy gaps. Underbrush within the ponderosa pine experiment site reached 1.5 m in height.

## 2.2. Experimental design

During the experimental trials, instruments were arrayed radially around the surrogate pheromone source at the ponderosa pine field site (Fig. 1); a very similar arrangement was used for the lodgepole pine site. During each field campaign, a total of nine experimental trials were carried out, one trial per day, each trial consisted of nine sequential 30-min sampling periods (totaling 4.5 h per day). To obtain data for a range of atmospheric conditions, the starting times varied from early morning to early afternoon. During each test day, SF<sub>6</sub> (1% mixture in air, Scott-Marrin Inc., Riverside, CA) was released continuously at a constant within-trial rate (see Section 2.4) from a point source located 1.4 m above the forest floor in the center of three concentric circles (Fig. 1). To examine plume characteristics in the near field, radii starting at the surrogate pheromone source and extending 5, 10, and 30 m were selected for the circles; SF<sub>6</sub> sampling devices were placed on these circles.

## 2.3. Instrumentation

At the beginning of every test, portable syringe sampler boxes (Krasnec et al., 1984) were arranged on the circles surrounding the surrogate pheromone source (Fig. 1). On the 5 m circle, the samplers were placed consistently every 30° and on the 10 and 30 m

circles, the samplers were placed every 15° or 30° and located so that the majority were downwind with a few on the upwind and crosswind side of the array. The arrangement of sampler boxes on the 10 and 30 m circles changed daily and placement depended on wind direction. Placing the samplers on the 10 and 30 m circles in a downwind configuration increased the likelihood of collecting surrogate pheromone concentration data as the plume meandered during the trial. The majority of the syringe samplers were positioned at 1.2 m above the forest floor, however, every 90° on the 10 and 30 m circles one or two additional samplers were placed at heights of 2.4 m and/or 7.5 m above the forest floor. Three additional samplers were located on a 27 m tower, located between 20 and 30 m from the source, one sampler near the forest floor, one in the midbole region, and one near the canopy top. One sampler box was located away from the experimental trial to collect background surrogate pheromone concentrations.

For each test, all of the syringe sampler boxes were loaded with nine syringes and programmed to start simultaneously and then pull each syringe sequentially at a preset rate of 30-min per syringe. Every syringe sampler box continuously collected samples for 4.5 h, filling the nine syringes. Each syringe represented a 30-min time-averaged data point. At the end of the experimental trial, the syringes were collected and analyzed within 24 h with a fast response continuous SF<sub>6</sub> analyzer (Benner and Lamb, 1985) equipped for rapid sample analysis.

To collect instantaneous concentrations at 1 Hz, a fast response SF<sub>6</sub> analyzer (Benner and Lamb, 1985) using an electron capture gas detector was located on the 10 m circle. The analyzer was placed on a cart so it could be moved along the 10 m circle to various downwind receptor points. Polyethylene tubing extended from the analyzer to a selected receptor point, usually at one of the syringe sampler locations, and instantaneous concentration data were collected at one location for 30-min. The detection limit of the analyzer was approximately 20 parts per trillion (ppt) and the detection range was 10 ppt to 10 ppb. The instrument was calibrated periodically during each test day with certified Scott-Marrin Inc. standards ( $\pm 5\%$  accuracy).

## 2.4. Surrogate pheromone release at the source

The SF<sub>6</sub> tracer was used as a surrogate pheromone and was released at the center of the experimental trial through polyethylene tubing 1.4 m above the ground. A mass flow controller (Tylan FC-260 Series, Tylan General, Rancho Dominguez, CA) placed between the compressed gas cylinder and tubing was used to insure a constant flow of SF<sub>6</sub>. Tracer release rates were adjusted and set for every trial to optimize plume detection at the furthest distance (30 m). Mean 30-min sampling period release rates ranged from 82 to 109  $\mu\text{g/s}$  and from 84 to 311  $\mu\text{g/s}$  for the lodgepole pine and ponderosa pine field studies, respectively (Table 2).

## 2.5. Meteorological measurements

Wind velocity components ( $u$ ,  $v$ , and  $w$ ) and temperature were measured with a sonic anemometer (K probe, ATI Inc., Longmont,

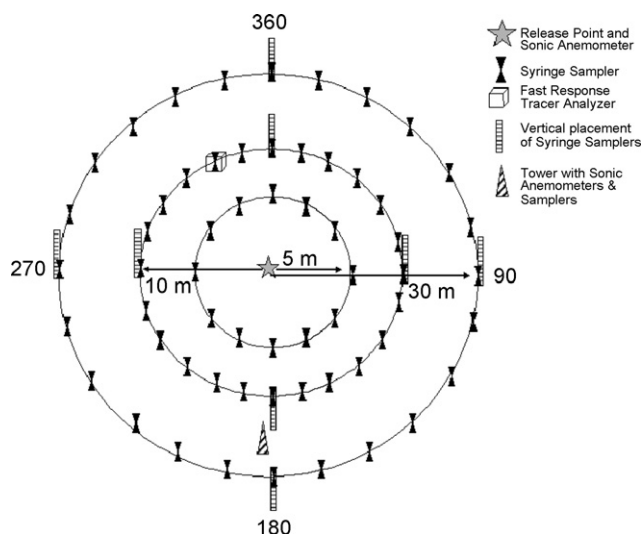


**Fig. 1.** Schematic of the tracer and meteorological deployment pattern (not to scale) for the ponderosa pine field campaign; all tracer studies were set up similarly. On the 5 m circle, the samplers were placed every 30° and on the 10 and 30 m circles the samplers could be placed every 15° or 30°, depending on the number available at the start of the experimental trial (all possible locations displayed). Samplers in the array were deployed at a higher density in downwind positions.

**Table 2**

Mean  $\pm$  S.E. surrogate pheromone (SF<sub>6</sub>) release rates, wind speed<sup>a</sup>, and temperature<sup>a</sup> during the daily experimental trials in a lodgepole pine stand (July 2000, Potomac, Montana)<sup>b</sup> and in a ponderosa pine stand (June 2001, LaPine, Oregon)<sup>b</sup>.

Date	Start time	Number of sampling periods (sample size)	Release rate ( $\mu\text{g/s}$ )	Wind speed (m/s)	Temperature ( $^{\circ}\text{C}$ )
Lodgepole pine site					
22 July 2000	11:30	9	101 $\pm$ 0.81	0.91 $\pm$ 0.04	27.9 $\pm$ 0.49
23 July 2000	04:30	9	82 $\pm$ 0.22	0.27 $\pm$ 0.01	9.2 $\pm$ 0.76
24 July 2000	04:30	9	82 $\pm$ 0.21	0.27 $\pm$ 0.01	9.7 $\pm$ 0.74
25 July 2000	08:00	9	105 $\pm$ 0.26	0.56 $\pm$ 0.05	23.2 $\pm$ 0.72
26 July 2000	06:30	9	108 $\pm$ 0.72	0.48 $\pm$ 0.08	14.9 $\pm$ 1.60
27 July 2000	06:30	9	102 $\pm$ 0.20	0.48 $\pm$ 0.08	18.7 $\pm$ 1.41
28 July 2000	06:30	9	107 $\pm$ 0.65	0.45 $\pm$ 0.07	15.6 $\pm$ 1.76
29 July 2000	06:30	9	108 $\pm$ 0.42	0.27 $\pm$ 0.02	13.7 $\pm$ 1.13
Ponderosa pine site					
20 June 2001	14:30	5	125 $\pm$ 0.10	0.89 $\pm$ 0.05	26.8 $\pm$ 0.25
21 June 2001	10:30	9	132 $\pm$ 9.14	0.96 $\pm$ 0.06	25.7 $\pm$ 0.31
22 June 2001	09:30	9	295 $\pm$ 0.84	0.90 $\pm$ 0.03	22.1 $\pm$ 0.84
23 June 2001	04:30	9	306 $\pm$ 0.54	0.56 $\pm$ 0.04	10.5 $\pm$ 0.50
24 June 2001	04:30	8	311 $\pm$ 0.13	0.45 $\pm$ 0.04	7.6 $\pm$ 0.12
25 June 2001	14:30	4	301 $\pm$ 0.12	0.62 $\pm$ 0.08	16.9 $\pm$ 0.12
26 June 2001	08:30	6	305 $\pm$ 0.56	0.51 $\pm$ 0.04	11.4 $\pm$ 0.52
27 June 2001	08:00	5	307 $\pm$ 0.30	0.64 $\pm$ 0.17	10.9 $\pm$ 0.28

<sup>a</sup> Meteorological data collected with the sonic anemometer (K probe, ATI Inc., Longmont, CO) located at the source. Trials with precipitation were not included in the analyses.

<sup>b</sup> Each field test lasted 4.5 h.

CO) located at the source. The anemometer was positioned 1.4 m above the forest floor and collected data continuously at 10 Hz throughout every trial. The high-frequency data collected by this anemometer (Table 2 for daily trial mean  $\pm$  S.E.) were used as 10 Hz input into the instantaneous dispersion model.

Three three-dimensional sonic anemometers (Vx probe, ATI Inc.) were deployed at three heights on the 27 m tower to measure turbulence and temperature profiles. The data from these anemometers were used to characterize the stability conditions during the sampling periods (Thistle et al., 2004). Additionally, two 7 m meteorological towers were deployed near the site to measure mean temperature, humidity, wind speed and direction and net radiation at two heights.

## 2.6. SF<sub>6</sub> as a pheromone surrogate

SF<sub>6</sub> is an inert, colorless, odorless, harmless gas that is easily measured with an electron capture detector. Detection of SF<sub>6</sub> can occur at very low concentrations, in the parts-per trillion range. This coupled with low background concentrations and minimal detector interference makes SF<sub>6</sub> an ideal tracer gas. SF<sub>6</sub> will not degrade quickly, and during the 30-min sampling time scale used in the experimental trials it remained intact. Insect pheromones will degrade chemically or photolytically but as long as the pheromones are not in the class of very reactive biogenic volatile organic compounds (VR-BVOC) that react in 1 min or less (Holzinger et al., 2004), they are most likely conserved over the short horizontal transport distances used in this study. For example, the slowest mean wind speed observed during the two studies was 0.27 m/s (Table 2), at this wind speed, mass released at the center of the largest experiment circle (with a radius of 30 m) will cross the perimeter of the circle within 2 min. Many terpenes similar in molecular structure to insect pheromones have reaction times on the order of 10–15 min (Lee et al., 2006a, 2006b). Additionally, SF<sub>6</sub> is a large molecule and at 146 g mol<sup>-1</sup> it is similar in molecular weight, although slightly smaller than most bark beetle pheromone molecules. Because turbulent transport is the dominant diffusion process in the atmosphere, we can assume that any conservative inert chemical species will move and spread in a similar fashion under a forest canopy (i.e., SF<sub>6</sub> and pheromone); thus SF<sub>6</sub> can be used as a surrogate pheromone for these conditions.

## 2.7. Reporting of data

To negate bias associated with different release rates, the 30-min time-averaged concentration data ( $\chi$ ) were normalized with the sampling period release rate ( $Q$ ). This allowed comparison of concentration data from the two different field study sites and across daily experimental trials. For every sampling period, there were three concentration maximums, one per circle, these arc maxima were used in the analyses below. Henceforth,  $\chi/Q$  will be used to represent the arc maximum normalized surrogate pheromone concentration. The arc maxima used in the following analyses provide a data set of single points that convey important mean plume behavior information. To explore the data in its true form, instantaneous concentrations are reported in parts per trillion (ppt) of SF<sub>6</sub>.

Meteorological and turbulence data reported below were recorded by the sonic anemometer located at the surrogate pheromone source. The 10 Hz data were averaged to 30-min wind speed vectors (m s<sup>-1</sup>) and used to calculate wind direction variance. Here, the term wind direction variance refers to that used by Thistle et al. (2004); it is the 30-min average of the lateral variance in the wind speed (m s<sup>-1</sup>) divided by the rotated 30-min wind speed vector average (m s<sup>-1</sup>). Water droplets on the sonic anemometer transducers can interfere with data collection; all sampling periods during which precipitation occurred were eliminated from the analyses.

## 3. Instantaneous dispersion model

A three-dimensional Lagrangian puff model was derived from the meandering plume model presented by Peterson et al. (1990), whose model was driven by high-frequency sonic anemometer data. The puff version of the model focuses on individual puff growth and spread and was developed to simulate instantaneous puff behavior while the puffs meander and spread acting as a plume in entirety. The three-dimensional 10 Hz wind velocity components collected by the sonic anemometer located at the surrogate pheromone source are the only model input. With this approach, it is assumed that turbulence mechanically generated from tree trunks and underbrush or thermally generated from canopy sun spots is inherently incorporated into the model via the sonic turbulence record.

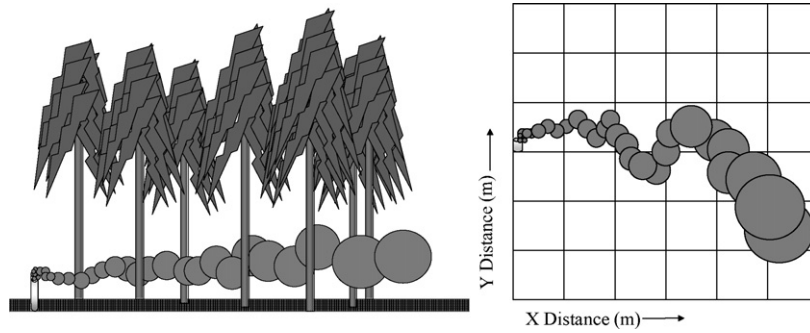


Fig. 2. Illustration of puffs simulated by the Lagrangian instantaneous puff model.

The instantaneous dispersion model simulates plume dispersion in terms of a continuous series of individual, overlapping puffs (Fig. 2). A puff is emitted from the simulated surrogate pheromone source every second. Once emitted the simulated puff is transported by the model in the  $x$ ,  $y$ , and  $z$  directions according to the 1 s time-averaged wind velocity components ( $u$ ,  $v$ , and  $w$ ). The 10 Hz  $u$ ,  $v$ , and  $w$  wind velocity data (collected by the on-site sonic anemometer) are averaged to 1 s data in the model. Instantaneous concentrations ( $\chi$ ) at a sampling point are modeled as the sum of the contributions from all individual puffs ( $X_{ip}$ ):

$$\chi = \sum_{P=1}^N X_{ip} \quad \text{where,} \quad (1)$$

$$X_{ip} = \frac{\dot{m}}{2\sigma_z\sigma_r^2\pi\sqrt{2\pi}} \left[ \exp\left(-0.5\left(\frac{r}{\sigma_r}\right)^2\right) \right] \times \left[ \exp\left(-0.5\left(\frac{z+H}{\sigma_z}\right)^2\right) + \exp\left(-0.5\left(\frac{z-H}{\sigma_z}\right)^2\right) \right] \quad (2)$$

where  $\dot{m}$  is the mass ( $\mu\text{g}$ ) released every second;  $r$  is the radial distance from the center of each puff to a specific receptor point (m);  $z$  is the height of the receptor above the surface (m);  $H$  is the release height (m);  $\sigma_r$  and  $\sigma_z$  are the horizontal and vertical dispersion coefficients of the puff (m); and  $N$  is the number of puffs impacting the receptor point.

The instantaneous puff dispersion coefficients were calculated for each puff with the following equations:

$$\sigma_r(t) = \sigma_r(t) + \Delta\sigma_r(t) \quad \text{where,} \quad (3)$$

$$\Delta\sigma_r(t) = (\sigma_u(t)^2 + \sigma_v(t)^2)^{1/2} \Delta t \quad (4)$$

$$\sigma_z(t) = \sigma_z(t) + \Delta\sigma_z(t) \quad \text{where,} \quad (5)$$

$$\Delta\sigma_z(t) = \sigma_w(t) \Delta t \quad (6)$$

where  $\sigma_u$ ,  $\sigma_v$ , and  $\sigma_w$  are the measured, short-term standard deviations of velocity from the sonic anemometer;  $t$  is puff travel time, and  $\Delta t$  is the 1-s time step used in the model. Instantaneous concentrations ( $\chi$ ), contributions from the individual puffs ( $X_{ip}$ ), and the dispersion coefficients ( $\sigma_r$  and  $\sigma_z$ ) are calculated every second. Puff contributions are calculated on a regular gridded array.

The domain and grid size were set to  $50\text{ m} \times 50\text{ m} \times 5\text{ m}$  and  $0.5\text{ m} \times 0.5\text{ m} \times 0.5\text{ m}$ , respectively. The domain was centered over the surrogate pheromone source and set to encompass the experimental trial. The simulated surrogate pheromone release rate was adjusted every 30-min to match the release rate used during the sampling period in the field.

### 3.1. Output—time-averaged concentrations

The model can be set to output time-averaged concentrations on a regular gridded array, covering the entire domain, or at specific locations within the domain. To compare simulated concentration data to observed concentration data, the model was set to output 30-min time-averaged concentrations at every possible syringe sample location; every  $30^\circ$  on the 5 m circle and every  $15^\circ$  on the 10 and 30 m circles. This insured simulated data at the location of the observed data. The simulated time-averaged concentration data were normalized with the sampling period release rate and the arc maximum concentrations were calculated.

### 3.2. Output—instantaneous concentrations

Instantaneous model output is a time series of 1 s surrogate pheromone concentrations at designated receptor points. The model was set to output the concentration time series at the location of the fast response analyzer, this location changed with sampling period, but was always on the 10 m circle. This simulated concentration time series can be compared directly to measured instantaneous surrogate pheromone concentrations obtained with the SF<sub>6</sub> analyzer.

## 4. Discussion of the experimental trials and atmospheric temperature

Occasionally, the experimental trials were conducted at temperatures below which or at times of the day when beetle flight does not occur (Table 2). This was done to measure dispersion over a range of conditions and to allow creation of a sufficiently generic in-canopy dispersion model. It is not the absolute temperature that is important to dispersion but, instead, temperature change with height ( $dT/dz$ ). The stability conditions, dependent on  $dT/dz$ , during times of lower temperatures may be similar to pre-storm conditions; bark beetles have been found to fly in high numbers just before late afternoon thunderstorms (Vité et al., 1964). The dispersion patterns found during the cooler tests can be applied to times of the day when warmer temperatures prevail, such as before a thunderstorm, as long as the stability pattern is similar.

## 5. Model results and discussion

In this section, to demonstrate model performance, the observed surrogate pheromone concentration data are presented alongside the simulated data. The companion paper, Thistle et al. (2004), reports and explores the meteorological and concentration observations in detail; here we are using the observation data to investigate the strengths and weaknesses of the model.

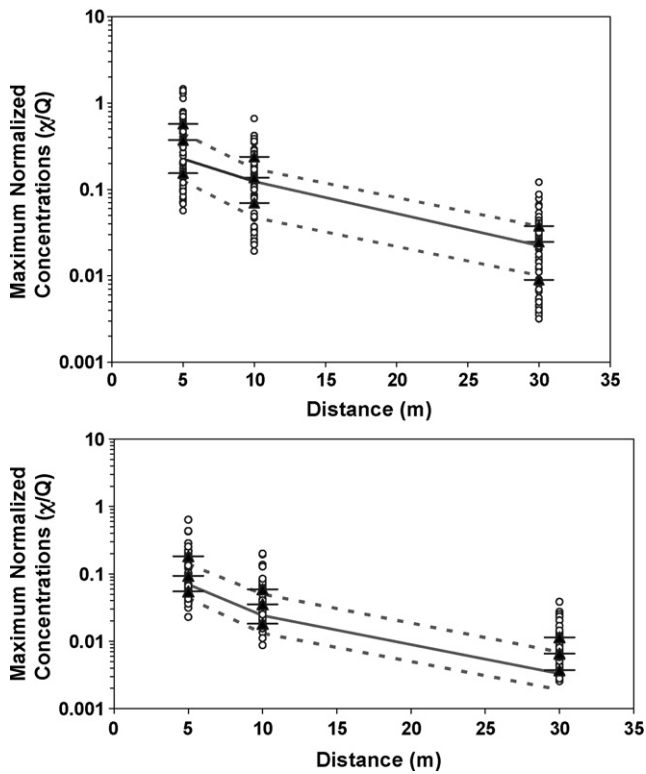


**Fig. 3.** Simulated  $\chi/Q$  [receptor concentration ( $\text{g m}^{-3}$ )/release rate ( $\text{g s}^{-1}$ )] maximum surrogate pheromone concentrations for the lodgepole pine (top) and ponderosa pine (bottom) canopies (circles), the predicted median and first and third quartiles are the black triangles with horizontal dashes. For comparison purposes the observed median (solid line) as well as the first and third quartiles (dashed lines) are shown.

5.1. Simulated mean plume behavior

To develop a general picture of mean plume behavior near the forest floor, Thistle et al. (2004) plotted observed  $\chi/Q$  [receptor concentration ( $\text{g m}^{-3}$ )/release rate ( $\text{g s}^{-1}$ )] vs. distance from the source, vs. 30-min mean wind speed, and vs. 30-min wind direction variance. For comparison purposes, we present similar figures with observed and simulated  $\chi/Q$  (Figs. 3–5). Best-fit curves used to analyze the potential to predict the observed and simulated data with respect to wind speed and wind direction variance were chosen based on the highest correlation between simulated  $\chi/Q$  and the independent variable. These figures are presented for comparison between simulated and observed data; we are not trying to infer statistical influence of the independent variable on the data. For brevity, the simulated and observed  $\chi/Q$  data from the 5 and 10 m circles were chosen to display trends with wind speed and wind direction variance, respectively. Simulated and observed  $\chi/Q$  from the 5, 10, and 30 m circles were calculated for all sampling periods (Appendix A).

Dilution of a concentration field increases with distance from the source, and as expected, simulated and observed  $\chi/Q$ , medians, and first and third quartiles decrease with increasing downwind distance (Fig. 3). Model results were somewhat higher than observed concentrations for both sites, 5 and 10 m from the source, and the overestimation of the simulated data was most pronounced for the ponderosa pine 30 m location, where the simulated median was near the observed third quartile. Curiously, the model did not overestimate concentrations for the lodgepole pine 30 m location, where the simulated  $\chi/Q$  median and first and third quartiles were very near the observed median and first and third quartiles. The

simulated rate of decreasing concentration with distance closely matched the observed rate of decrease at both sites.

Wind speed is the predominant factor in transporting pheromone from a source to a receptor. Higher wind speeds lead to lower simulated and observed surrogate pheromone concentrations (Fig. 4). At the 5 m location, the  $\chi/Q$  simulated by the model produced the power law trend that the observed  $\chi/Q$  demonstrate when plotted against 30-min mean wind speeds. The correlation between the lodgepole pine simulated concentrations and mean wind speed was slightly lower than the correlation between the observed concentrations and mean wind speed, the inverse was true for the ponderosa pine site. The constants in the observed and simulated regression equations were very similar and, in general, the model simulated the trend associated with concentrations and mean wind speed.

Wind direction variance is a measure of plume meander; as the wind direction variance increases; time-averaged maximum concentrations decrease (Fig. 5). This is demonstrated when comparing the data from the lodgepole pine site, where wind direction varied little during many of the sampling periods and the corresponding 10 m  $\chi/Q$  were elevated, to data from the ponderosa pine site, where wind direction varied greatly, resulting in low 10 m  $\chi/Q$ . The model simulated this trend between  $\chi/Q$  and wind direction variance. At both sites, the simulated  $\chi/Q$  arc maxima had a better degree of correlation with wind direction variance compared to the observations. This is to be expected since the model only considers wind direction and speed measured at a single location and does not directly take into account surface roughness, the effects of tree

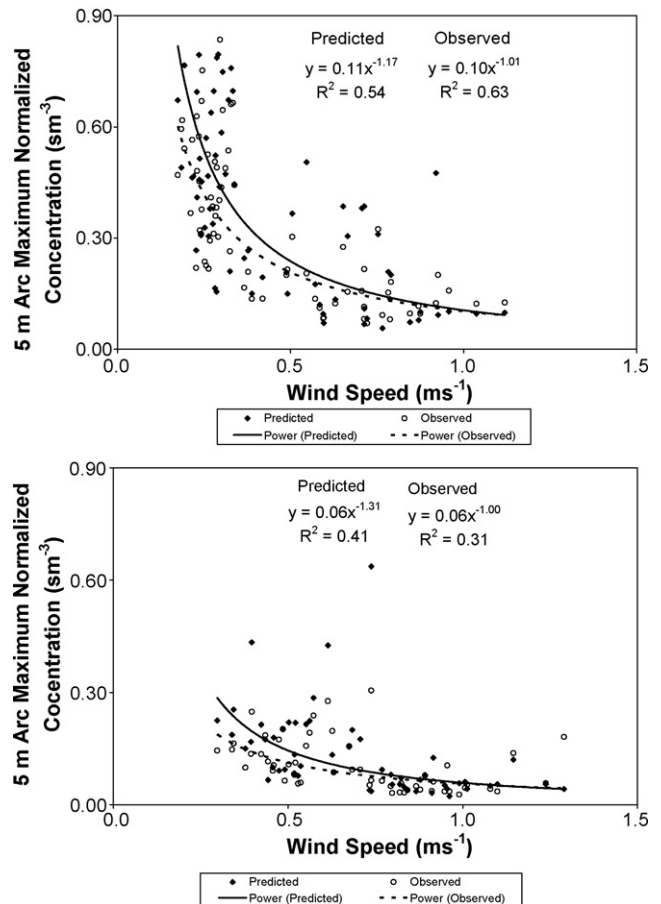


**Fig. 4.** Simulated and observed  $\chi/Q$  [receptor concentration ( $\text{g m}^{-3}$ )/release rate ( $\text{g s}^{-1}$ )] maximum surrogate pheromone concentrations on the 5 m circle vs. mean wind speed for the lodgepole pine (top) and ponderosa pine (bottom) sites.

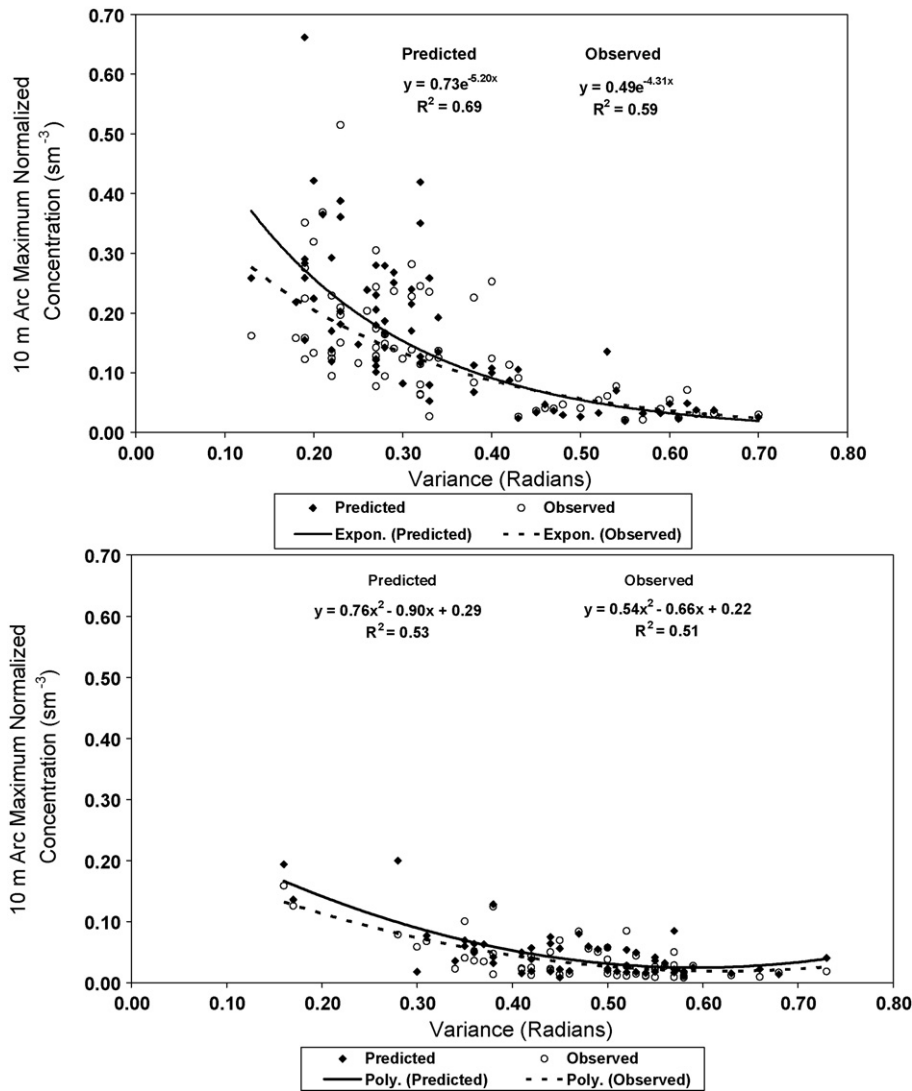


Fig. 5. Simulated and observed  $\chi/Q$  [receptor concentration ( $\text{g m}^{-3}$ )/release rate ( $\text{g s}^{-1}$ )] maximum surrogate pheromone concentrations 10 m from the source plotted against wind direction variance for the lodgepole pine (top) and ponderosa pine field (bottom) campaigns.

trunks on plume mixing, nor the effects of spatially variable forest floor heating, due to sun flecking, upon vertical motion.

Observed vertical profiles of the time-averaged data were difficult to ascertain due to dilution of the plume and a minimal number of samplers used to collect data above 1.2 m. Comparison of model results (domain set to  $50 \text{ m} \times 50 \text{ m} \times 10 \text{ m}$  for these simulations) to the vertical distribution of surrogate pheromone at the cardinal locations on the 10 m circle showed reasonable results (Fig. 6). The predicted and observed vertical gradients were similar and the ranges of concentrations at each level were similar.

Simulated and observed concentration shapes at 1.2 m above the forest floor for the 5 and 10 m circles demonstrate model performance with respect to location (Fig. 7). Resemblance between the two concentration shapes varies with sampling period from excellent (Fig. 7a, b, and f) to acceptable (Fig. 7g, h, and i). The model is able to simulate basic shapes (Fig. 7a–f) but does not do well capturing the more complex concentration structure (Fig. 7g–j).

## 5.2. Model performance statistics

Paired (in time) model performance statistics were calculated to quantify overall model performance (Table 3). The mean bias (MB), mean error (ME), fractional bias (FB), and fractional error (FE) were

obtained using the  $\chi/Q$  arc maxima:

$$\text{MB} = \frac{1}{N} \sum_{1}^N C_m - C_o \quad (7)$$

$$\text{ME} = \frac{1}{N} \sum_{1}^N |C_m - C_o| \quad (8)$$

$$\text{FB} = \frac{1}{N} \sum_{1}^N \frac{C_m - C_o}{(C_m + C_o)/2} \quad (9)$$

$$\text{FE} = \frac{1}{N} \sum_{1}^N \frac{|C_m - C_o|}{(C_m + C_o)/2} \quad (10)$$

where  $C_m$  and  $C_o$  are the modeled and observed concentrations, respectively.

The MB and ME return values in units, whereas the FB and FE are reported in percentages. The bias terms convey overall model tendencies while the error terms give the average error between modeled and observed values (Boylan and Russell, 2006). A positive or negative value from MB or FB demonstrates an overall trend

**Table 3**

Model performance statistics for  $\chi/Q$  [receptor concentration ( $\text{g m}^{-3}$ )/release rate ( $\text{g s}^{-1}$ )], normalized maximum surrogate pheromone concentrations for the lodgepole pine stand (July 2000, Potomac, Montana) and the ponderosa pine stand (July 2001, LaPine, Oregon).

Distance from source (m)	Lodgepole pine site			Ponderosa pine site		
	5	10	30	5	10	30
Mean bias ( $\text{s m}^{-3}$ )	0.10	0.02	0.00	0.03	0.01	0.00
Mean error ( $\text{s m}^{-3}$ )	0.14	0.05	0.01	0.05	0.01	0.01
Fractional bias (%)	17	10	-16	15	21	47
Fractional error (%)	35	33	52	39	38	69
Fa <sub>2</sub> (%)	83	90	65	87	85	53

for the model to over- or under-predict. The FB and the FE are normalized with the average of the modeled and the observed; this acknowledges error associated with both datasets and recognizes that the observations are not absolute truth (Boylan and Russell, 2006). Obviously as the sum of the modeled and observed values approaches zero the FB and FE performance metrics become less valuable. The FB and FE give equal weight to under-predictions and over-predictions and range from  $\pm 200\%$  and 0 to 200%, respectively (Seigneur et al., 2000). The fraction of the time the model simulated the  $\chi/Q$  within a factor of 2 of the observed  $\chi/Q$  (Fa<sub>2</sub>) was also calculated (Table 3).

The model correctly simulated the mean quantities; the MB and ME were small at all locations at both sites. The FB was low at the

lodgepole pine site, less than 17% for all distances, but the model over-predicted at the 5 and 10 m locations and under-predicted at the 30 m location. At the ponderosa site, the model over-predicted at all locations, with FB equal to 15% at 5 m and increasing with distance to 47% at 30 m. The FB has a range of  $\pm 200\%$  and an ideal value of 0, based on this performance metric, the model does exceptionally well for the lodgepole pine site and performs satisfactorily for the ponderosa pine site. The performance metric, FE ranged from 33% (10 m, lodgepole pine site) to 69% (30 m, ponderosa pine site). The FE results demonstrated satisfactory model performance at the 5 and 10 m locations and, although it was high for the 30 m locations, it was not unreasonable. The Fa<sub>2</sub> values reflect the trends demonstrated by the FE; best model performance occurred at the 5 and 10 m locations and reasonable model performance at the 30 m locations. Overall, the model did well in predicting the time-averaged surrogate pheromone  $\chi/Q$ .

The instantaneous puff dispersion model was applied to simulate a point source located near the surface below a tall canopy. Model performance of mean plume behavior is similar to that reported in the literature. Models designed to simulate instantaneous fluctuations reported in the literature have generally been tested against observation data collected downwind from a point source, located near the surface or on a tall stack, and above a short canopy, such as grass fields (Peterson and Lamb, 1992; Peterson and Lamb, 1995) and urban cover (Davakis et al., 2001). The filament-based model, described by Farrell et al. (2002), overestimated the downwind in-plume mean concentration data. Simulated concentrations produced by a Gaussian puff model, RIM-PUFF (Thytkier-Nielsen and Mikkelsen, 1993) were generally higher than observed concentrations at a long distance from the source in complex terrain (Brücher et al., 1998). Davakis et al. (2001) reports arc maximum statistics for the dispersion over complex terrain model (Davakis et al., 2000) with Fa<sub>2</sub> values ranging from 47% to 49%, their sample size was much larger ( $N = 1216$ ) compared to the sample sizes from the lodgepole ( $N = 72$ ) and ponderosa ( $N = 55$ ) sites.

To provide a frame of reference for how FB and FE are used to evaluate model performance, we site the FB and FE model performance goals and criteria set forth by the US Environmental Protection Agency for fine particulate matter (PM<sub>2.5</sub>). Fractional bias and error goals and criteria are based on availability of current and future technology (US EPA, 2007). The established goals and criteria for PM<sub>2.5</sub> for FB is  $\pm 30\%$  and  $\pm 60\%$ , respectively, and FE  $\leq 50\%$  and  $\leq 75\%$ , respectively (Boylan and Russell, 2006). We can use these model performance goals and criteria to gain a relative understanding of model performance described here. The simulated surrogate pheromone concentrations meet the FB goal at all locations for the lodgepole pine site and at the 5 and 10 m locations for the ponderosa pine site. Model performance at the ponderosa pine 30 m location falls within the FB criterion. For both sites, at the 5 and 10 m locations, the FE goal is achieved and at the 30 m locations the simulated concentration data fall within the FE criterion.

An additional tool to assess model performance is the quantile–quantile (Q–Q) plot (Figs. 8 and 9); this type of plot

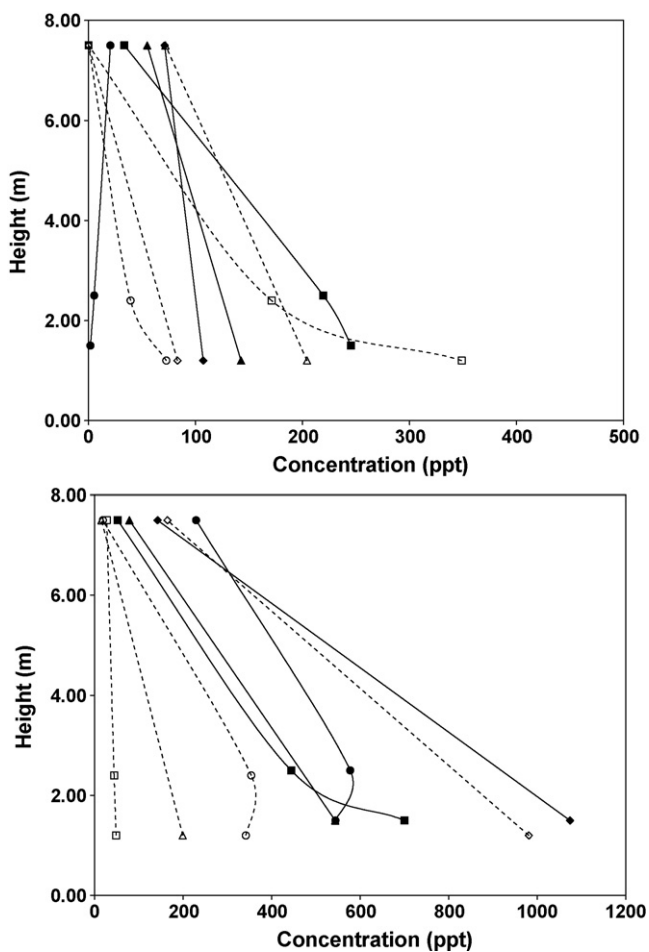


**Fig. 6.** Simulated (filled shapes with solid lines) and observed (open shapes with dashed lines) vertical profiles at the four cardinal directions (0° diamonds; 90° squares; 180° triangles; 270° circles) on the 10 m circle for the ponderosa pine site on 21 June 2001, 12:30 p.m. to 1:00 p.m. (top) and on 25 June 2001, 4:00 p.m. to 4:30 p.m. (bottom). To simulate the vertical concentration profiles, the domain height was set to 10 m and the vertical grids to 0.5 m.

**Table 4**  
 Simulated (s) and observed (o) mean ( $M$ ), maximum ( $Mx$ ), and minimum ( $Mn$ ) normalized arc maximum surrogate pheromone concentrations ( $\chi/Q$ ) under different canopy types. The ratios of simulated-to-observed are also included.

Distance from source (m)	$M_s$ ( $s\ m^{-3}$ )	$M_o$ ( $s\ m^{-3}$ )	$M_s/M_o$	$Mx_s$ ( $s\ m^{-3}$ )	$Mx_o$ ( $s\ m^{-3}$ )	$Mx_s/Mx_o$	$Mn_s$ ( $s\ m^{-3}$ )	$Mn_o$ ( $s\ m^{-3}$ )	$Mn_s/Mn_o$
Lodgepole pine									
5	0.424	0.320	1.33	1.463	0.835	1.75	0.057	0.070	0.81
10	0.165	0.142	1.16	0.662	0.515	1.29	0.019	0.021	0.90
30	0.027	0.032	0.84	0.121	0.111	1.09	0.003	0.003	1.00
Ponderosa pine									
5	0.134	0.103	1.30	0.637	0.305	2.09	0.023	0.027	0.85
10	0.046	0.037	1.24	0.200	0.159	1.26	0.009	0.008	1.13
30	0.009	0.007	1.29	0.039	0.054	0.72	0.003	0.000	–

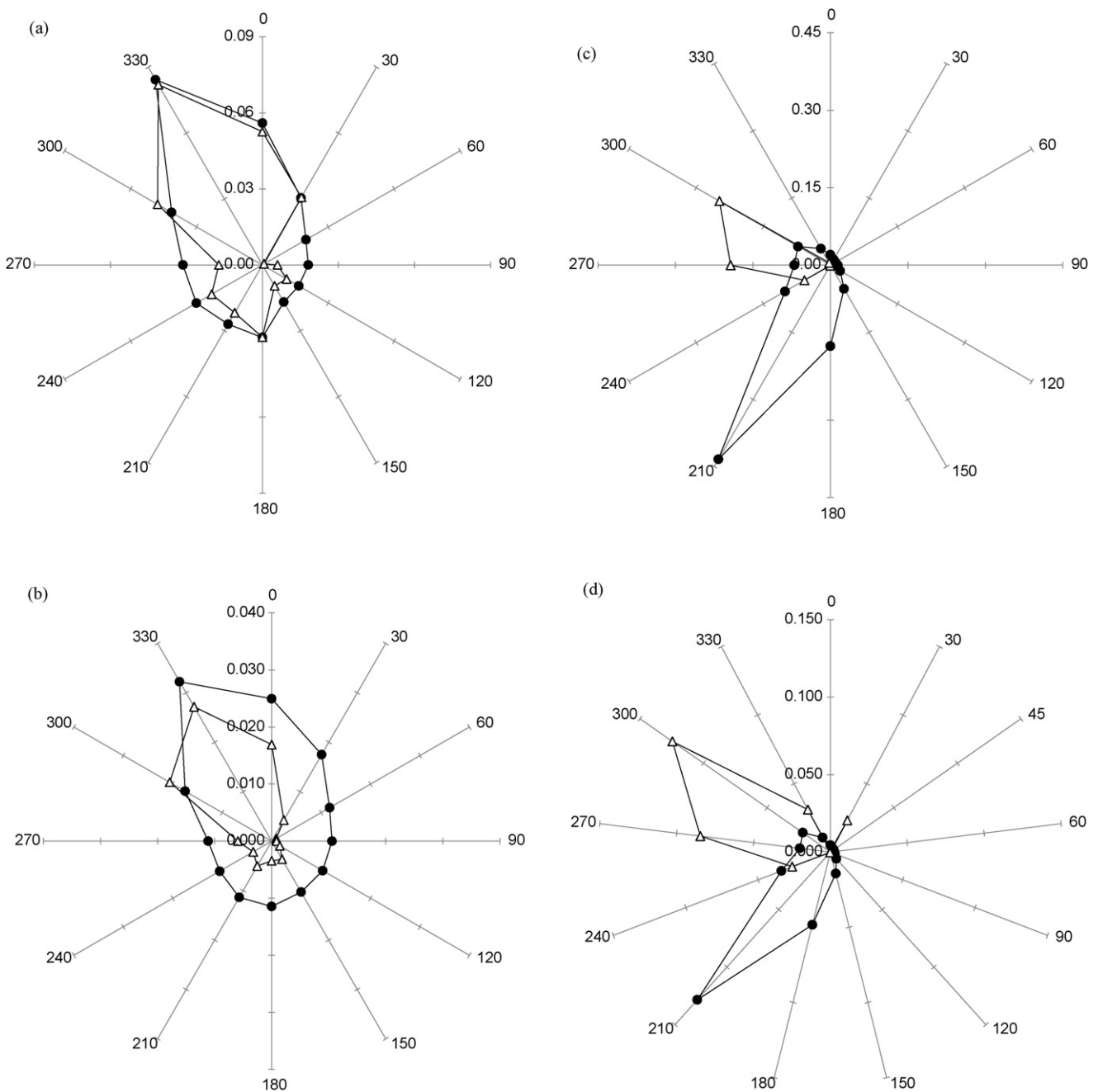


**Fig. 7.** Simulated (filled circles) and observed (open triangles) concentration shapes 1.2 m above the forest floor at 5 m (a, c, e, g, and i) and 10 m (b, d, f, h, and j) from the source for five cases selected from the ponderosa pine data.

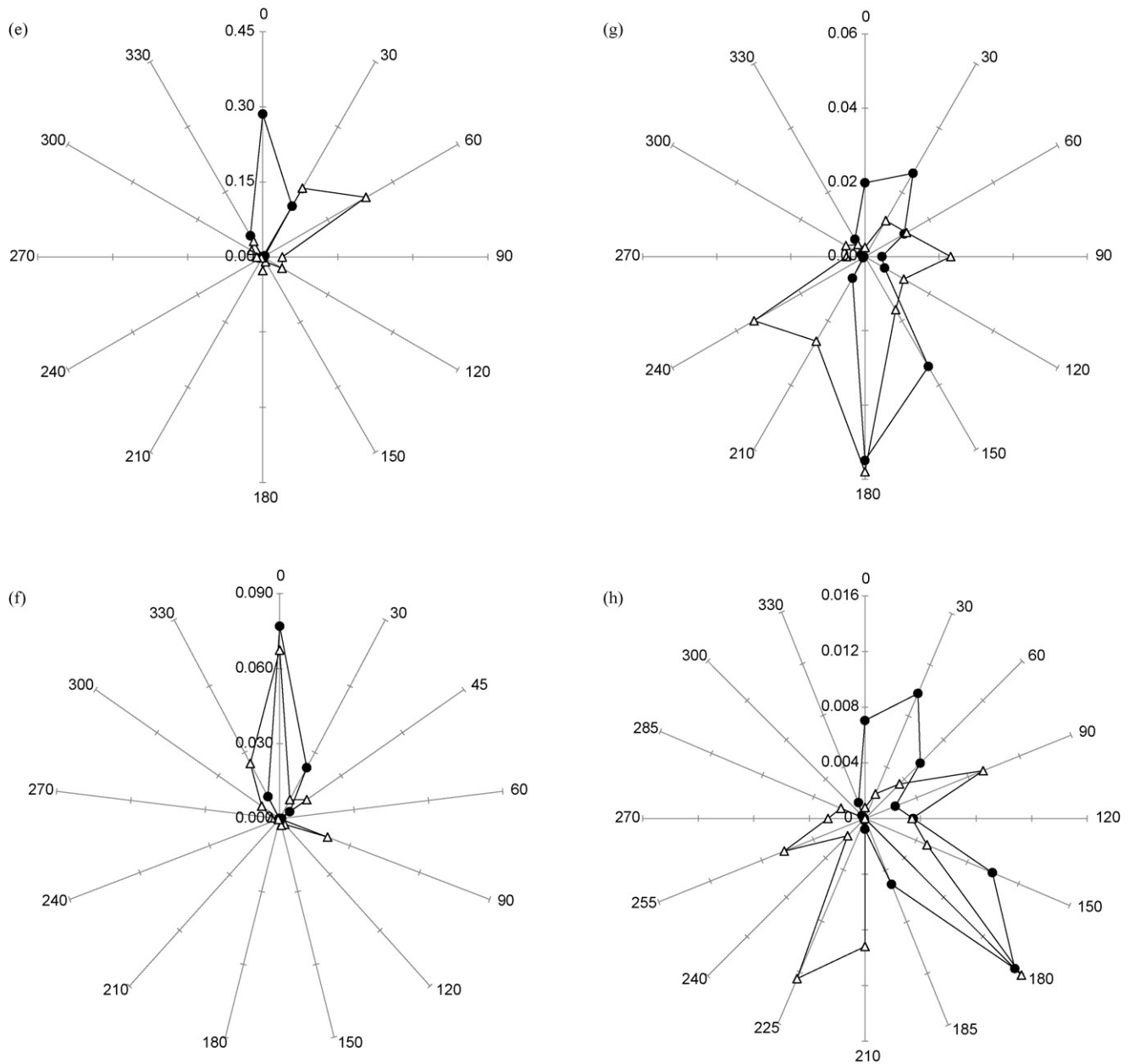


Fig. 7. (Continued).

demonstrates similarity between data set frequency distributions. If the modeled and observed data sets have a similar distribution the data will fall along a 1:1 line (Wilks, 2006), above or below the 1:1 line indicates model over- or under-prediction (Venkatram et al., 2001). The data are paired by sorting each data set, largest to smallest, making the data indeterminate in time. The overall tendency of the instantaneous dispersion model is displayed in the Q–Q plots by plotting the simulated  $\chi/Q$  data distribution with respect to the observed  $\chi/Q$  data distribution.

The Q–Q plot results are similar to the statistical FB results. For the lodgepole pine site the model over-predicted the concentrations at the 5 and 10 m locations and under-predicted concentrations at the 30 m location (Fig. 8). At all lodgepole pine locations the simulated data were within a factor of 2 of the observed data and for smaller concentrations the data lie on or very near the 1:1 line. Better model performance results were obtained at 10 m compared to the 5 and 30 m locations, however, all three plots show the simulated concentrations having

relatively the same distribution shape as the observed concentrations. For the ponderosa site, the simulated data show a similar distribution shape to the observed at the 5 and 10 m locations but show a difference at the 30 m location (Fig. 9). At the 5 and 10 m locations the model simulated the concentration data to within a factor of 2 of the observed data, the model performed slightly better at the 5 m location than at the 10 m. The model did not perform nearly as well at the ponderosa pine 30 m location compared to all other ponderosa pine and lodgepole pine locations.

### 5.3. Comparison of model performance between distance and canopies

The difference in magnitude between the 5, 10 and 30 m locations, as well as the different scales between the lodgepole and ponderosa pine sites becomes obvious when the concentration data are plotted in the Q–Q plots (Figs. 8 and 9). For both sites, the

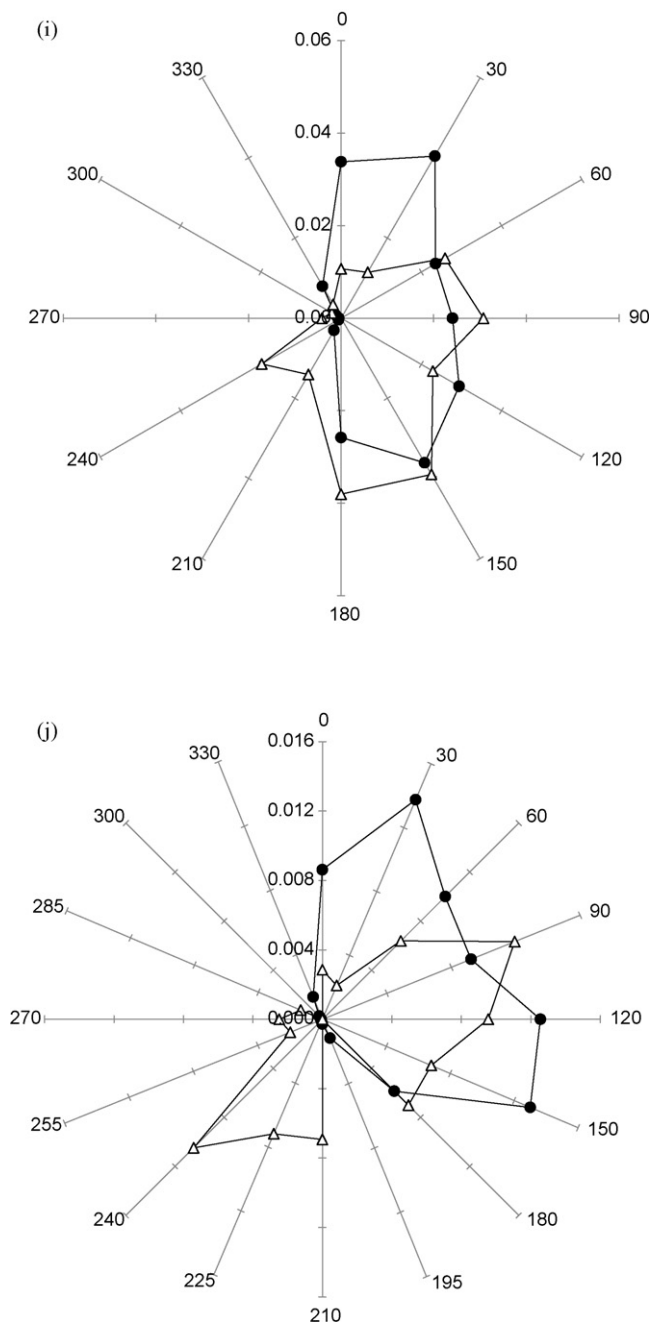


Fig. 7. (Continued).

observed maximum concentration occurs 5 m from the surrogate pheromone source (Fig. 3). The lodgepole pine site maximum is over twice the ponderosa pine site maximum, and the model matched this difference. The observed  $\chi/Q$  decrease in magnitude between the 5, 10, and 30 m locations for the mean, maximum and minimum values was also matched by the simulated data (Table 4).

Model performance did not differ between the lodgepole and ponderosa pine sites for the 5 m location and varied only slightly for the 10 m location, however performance behavior was opposite in sign for the 30 m location (Table 3). We speculate variation in canopy metrics (Table 1; Thistle et al., 2004) may account for majority of the difference in model performance, magnitude and sign, at the 30 m location. The dense and homogeneous lodgepole pine canopy uniformly dissipates energy to the forest floor (Finnigan, 2000). This uniform dissipation of large eddies allows

for measurement of wind velocity in a single location, at the surrogate pheromone source, to represent turbulence and mean wind speed at large distances ( $\leq 30$  m). The wind velocity data used as input into the model is representative of the lodgepole pine flow regime within the confines of the experimental trial. The large gaps and underbrush in the ponderosa pine forest could influence the turbulent flow field in a manner that is not characterized by turbulence measurements taken at a single location. Sunlight heats the forest floor through the canopy gaps and vertical motion develops as warm air near the floor rises, these vertical eddies can transport the surrogate pheromone out the canopy top. The underbrush can mechanically break down large eddies, changing the turbulent field. The ponderosa pine experimental trial was not centered in a canopy gap nor near underbrush, therefore thermal or mechanical turbulence produced by these features were not inherent in the sonic anemometer record. It is probable that this is the reason

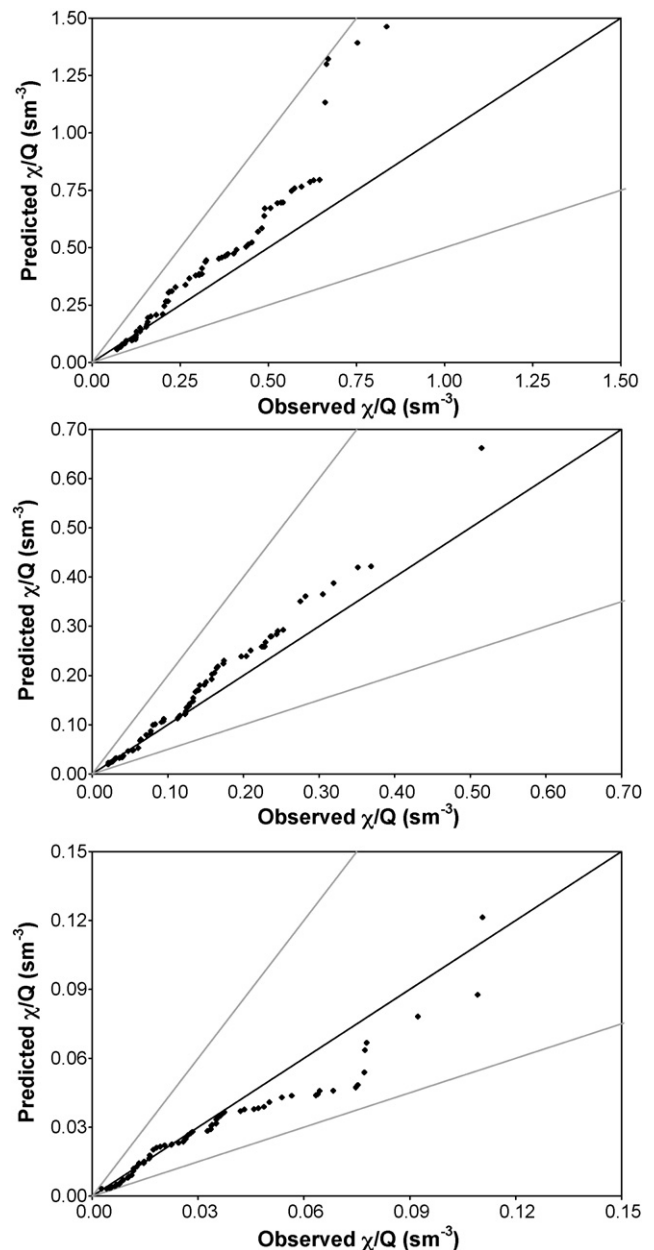


Fig. 8. Quantile-quantile plots (with 1:1 (dark) and 2:1 and 1/2:1 (light) lines) for 5 m (top), 10 m (middle), and 30 m (bottom) from the source at the lodgepole pine site.

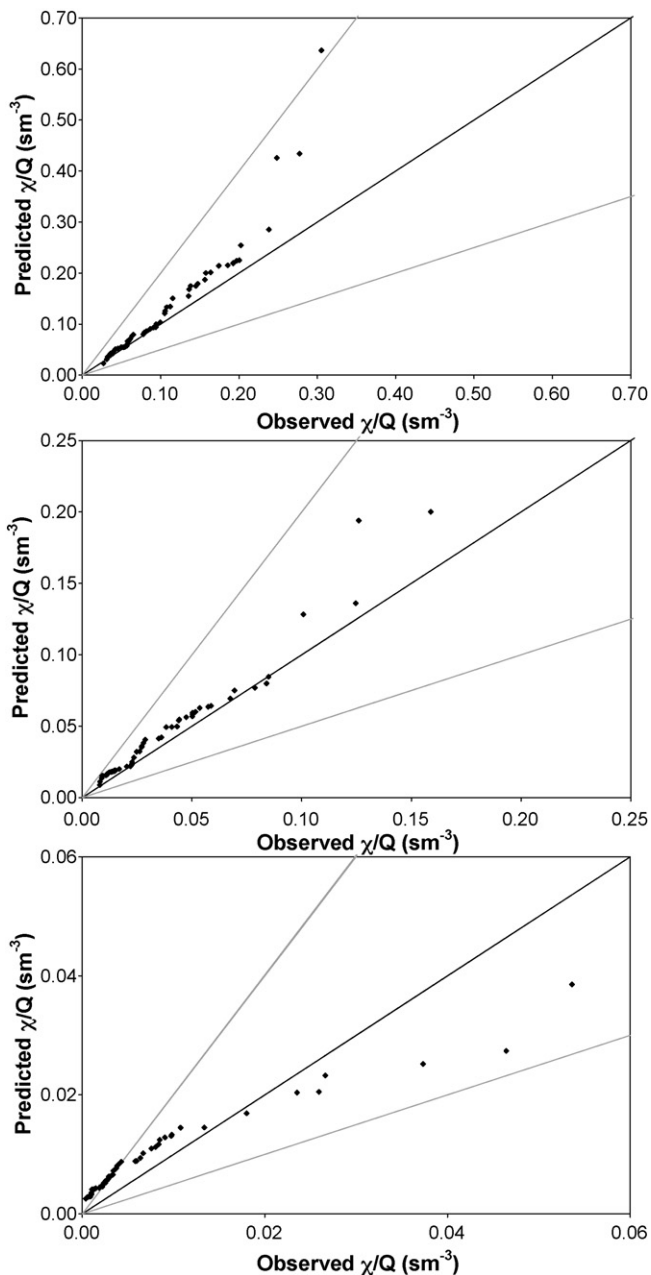


Fig. 9. Quantile-quantile plots (with 1:1 (dark) and 2:1 and 1/2:1 (light) lines) for 5 m (top), 10 m (middle), and 30 m (bottom) from the source at the ponderosa pine site.

for the higher 30 m FB at the ponderosa pine site, indicating model over-simulation. During a 30-min sampling period, by the time the plume was 30 m downwind, it is likely the plume meandered into a canopy gap or encountered underbrush and was further diluted through turbulent processes.

The model sufficiently simulated the mean plume behavior with respect to distance, wind speed, and wind direction variation, performing well with respect to these variables. Simulation of plume concentration shape at the 5 and 10 m circles varied from adequate to excellent, the model had difficulty producing the complex shapes observed in the data. The assumption that the sonic anemometer data collected in one location represents the turbulent field throughout the experimental array (radius  $\leq 30$  m) holds for the lodgepole pine site. This assumption begins to collapse at distances greater than 10 m from the surrogate pheromone source at the pon-

derosa pine site. The simulated concentrations display the same decrease in magnitude with distance as the observations and the simulated  $\chi/Q$  mean is within 32% of the observed  $\chi/Q$  mean at all distances for both sites (Table 4).

#### 5.4. Instantaneous plume behavior

Continuous surrogate pheromone concentrations measured at 1 Hz at various locations along the 10 m circle (Fig. 10) illustrate instantaneous plume structure and meander. Model performance for instantaneous plume behavior cannot be directly compared to the simulated or observed time-averaged data. The instantaneous concentrations (ppt) are presented for one location on the 10 m circle and represent a sequence in time, while the time-averaged results are reported in terms of arc maximum normalized concentrations. The observed instantaneous concentrations may or may not have been measured at the arc maximum location.

Characteristically, the surrogate pheromone plumes measured by the analyzer are intermittent with high peaks and narrow widths that result in high peak-to-mean ratios during the 30-min sampling period (Table 5). Murlis et al. (2000) observed intermittent concentrations and high peak to mean ratios in both their forest and open field ion tracer studies as did Peterson et al. (1990) in their open field SF<sub>6</sub> tracer studies.

Seven sampling periods from the lodgepole pine study and 13 from the ponderosa pine study were selected for model simulation of instantaneous concentrations. The sampling periods were selected based on completeness of the observation data. The concentration fluctuation intensity, intermittency, peak, peak-to-mean ratio, mean, and standard deviation were calculated to evaluate the simulated instantaneous concentrations (Table 5). These statistics demonstrate instantaneous and mean plume characteristics at a single point. The concentration fluctuation intensity is the standard deviation normalized by the mean and is used to demonstrate the turbulent fluctuations in the plume (Santos et al., 2005). The intermittency is the fraction of time the plume is impacting the sensor. These two plus the peak and peak-to-mean ratio demonstrate the instantaneous nature of the plume.

The model correctly simulated concentration fluctuation intensity; the results were within a factor of 2 of the observed concentration fluctuation intensities 86% and 77% of the time for the lodgepole and ponderosa pine sites, respectively. The intermittency of the simulated data was similar to the observed data, the model performed well for the lodgepole pine canopy, and adequately for the ponderosa pine canopy. Model performance was similar to the meandering plume models presented by Peterson and Lamb (1992) and Reynolds (2000b); both models were able to simulate intensity and intermittency within a factor of 2 for the majority of the cases.

Simulated peaks were generally less than observed peaks, however a handful of peaks were overestimated by the model, and these were at least double the observed peaks. The peak-to-mean ratio was satisfactory, 86% of the lodgepole pine and 55% of the ponderosa pine peak-to-mean ratios were within a factor of 2 of the observed peak-to-mean ratios. The peak-to-mean ratio results for the lodgepole and ponderosa pine sites are similar to the results from the meandering plume model with modified empirical equations to simulate dispersion (Peterson and Lamb, 1995). The instantaneous puff dispersion model did well in simulating the timing of the individual peaks for both sites (Fig. 10).

Model performance for mean and standard deviation of the instantaneous concentrations, was poor, over- and underestimating at the lodgepole pine site and mainly underestimating at the ponderosa site. These results differ from Peterson and Lamb (1995) who found excellent agreement between simulated and observed

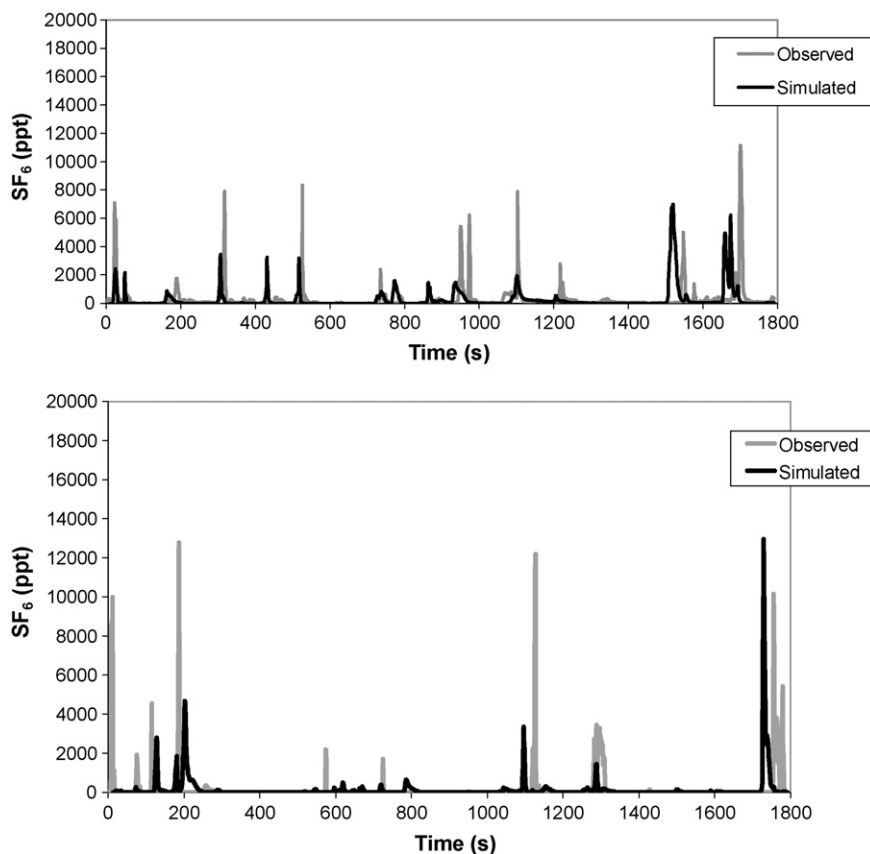


**Fig. 10.** Simulated and observed instantaneous data at the lodgepole site (top) at 10 m, 180°, on 24 July 2000, 10:00 a.m. to 10:30 a.m. and at the ponderosa pine site (bottom) at 10 m 225°, on 22 June 2001, 1:00 p.m. to 1:30 p.m.

mean concentrations of the instantaneous data. These differing results may be due to different treatments of the dispersion coefficients or it may be due to using only sonic anemometer data to drive all mechanics of puff development, transport, and dispersion. Given the simplicity of the model, the overall results are quite good.

### 5.5. Deployment of multiple sources

Most pheromone deployments involve the distribution of a number of artificial sources such as those used for beetle population monitoring (Erbilgin et al., 2002; Aukema et al., 2005), dispersal assessment (Turchin and Thoeny, 1993), and mass

**Table 5**  
Simulated (s) and observed (o) concentration fluctuation statistics<sup>a</sup>; concentration fluctuation intensity ( $I$ ), intermittency ( $i$ ), peak ( $P$ ), peak to mean ratio ( $P/M$ ), mean ( $M$ ), and standard deviation (S.D.), for the lodgepole pine (top) and the ponderosa pine (bottom) sites at a receptor located 10 m downwind from the source.

Date	Time	$I_s$	$I_o$	$i_s$	$i_o$	$P_s$ (ppt)	$P_o$ (ppt)	$P_s/M_s$	$P_o/M_o$	$M_s$ (ppt)	$M_o$ (ppt)	S.D. <sub>s</sub> (ppt)	S.D. <sub>o</sub> (ppt)
<b>Lodgepole pine</b>													
24 July 2000	07:00	4.9	4.2	0.18	0.25	88,810	12,704	40	27	2234	468	11,042	1952
24 July 2000	08:00	7.3	3.2	0.05	0.15	121,220	7,848	85	23	1427	340	10,459	1073
24 July 2000	10:00	3.0	3.2	0.41	0.75	6,975	11,148	28	36	252	307	759	982
24 July 2000	10:30	3.2	3.1	0.49	0.43	6,773	7,873	36	31	187	254	601	798
25 July 2000	08:00	7.9	7.4	0.03	0.07	4,402	15,286	95	80	46	192	368	1421
25 July 2000	08:30	1.6	2.2	0.76	0.59	11,436	12,289	9	18	1261	699	2,080	1538
27 July 2000	09:00	2.2	2.6	0.62	0.48	41,515	11,660	14	15	2987	758	6,453	1964
<b>Ponderosa pine</b>													
20 June 2001	15:00	4.7	4.2	0.19	0.12	10,003	11,343	75	46	133	245	630	1039
21 June 2001	12:00	2.0	3.8	0.56	0.26	3,869	9,980	13	43	306	231	604	871
21 June 2001	12:30	2.3	3.0	0.44	0.33	5,979	12,434	26	31	230	396	537	1199
21 June 2001	13:00	4.2	4.1	0.23	0.17	2,724	10,798	48	47	56	230	235	942
22 June 2001	10:30	3.8	4.1	0.42	0.20	20,990	12,025	46	37	454	322	1,710	1325
22 June 2001	11:30	3.4	9.4	0.38	0.07	11,172	14,070	43	307	261	46	883	432
22 June 2001	13:00	5.9	5.5	0.05	0.11	438	12,707	69	80	6	158	37	866
22 June 2001	13:30	12.1	3.8	0.19	0.18	21,550	7,253	336	33	64	223	780	840
23 June 2001	06:00	4.5	1.8	0.35	0.43	74,098	18,842	63	8	1176	2350	5,319	4292
24 June 2001	06:30	3.9	2.5	0.27	0.76	60,308	13,425	56	14	1085	943	4,240	2341
24 June 2001	07:30	4.8	2.5	0.22	0.38	5,141	12,736	48	15	108	856	519	2158
24 June 2001	08:00	4.5	2.7	0.19	0.27	2,061	5,134	73	22	28	232	128	637
26 June 2001	10:00	3.0	1.6	0.40	0.69	1,090	12,025	24	7	46	1766	139	2779

<sup>a</sup> Calculated from 30-min of observed and simulated 1 Hz data.

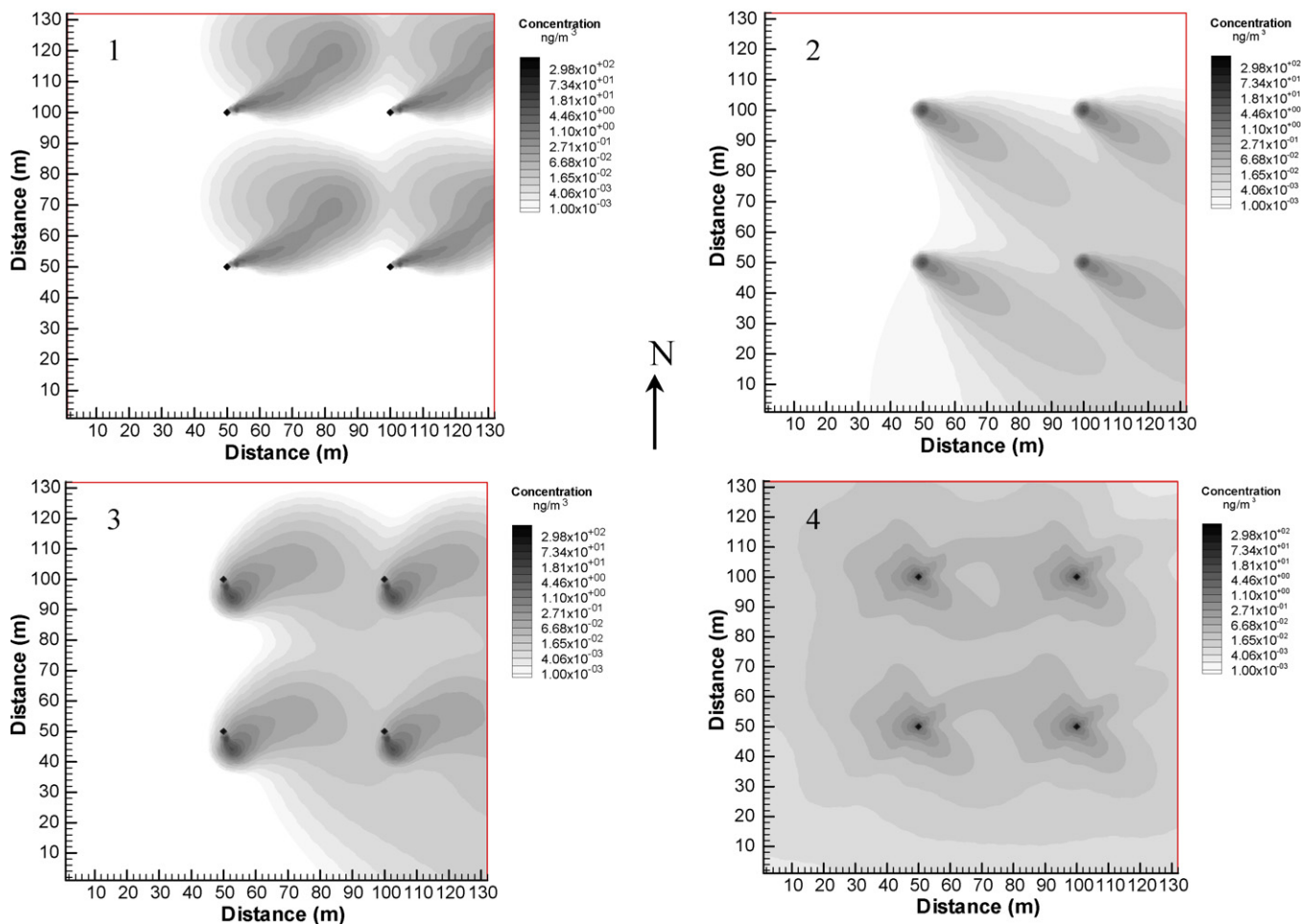


**Fig. 11.** Multiple pheromone source deployment simulation at the ponderosa pine site, each black diamond represents an ipsdienol (bark beetle pheromone) source releasing at a rate of  $0.0017 \mu\text{g/s}$ . Sonic data from the ponderosa pine site gathered on 22 June 2001 from 12:00 pm to 12:30 pm were used in the simulation. Panels 1, 2, and 3 represent 1-s concentration contours at 60, 600, and 1200 s into the simulation, respectively. Panel 4 represents the 30-min average concentration contour plot.

trapping (Lanier, 1979; Raty et al., 1995; Ross and Daterman, 1997) and for moth mating disruption (Tcheslavskaja et al., 2005). To show the concentration field for this type of multiple source deployment, the puff model was used to simulate four sources of the bark beetle pheromone component ipsdienol (Seybold and Vanderwel, 2003), in which each source has a strength of  $0.0017 \mu\text{g/s}$  over a 30-min period (Fig. 11). Racemic ipsdienol is a synthetic semiochemical used to mimic an attractant produced by the male bark beetle *Ips pini*. The release rate (measured in the laboratory at  $25^\circ\text{C}$ ) is provided by the manufacturer, Pherotech International Inc. (Delta, B.C., Canada). The sonic data from the ponderosa pine site were used; the data were recorded from 12:00 p.m. to 12:30 p.m. on a clear day in June. Results are shown as four panels; panels 1, 2, and 3 show 1-s concentration contours at 60, 600, and 1200 s into the simulation. Note that there is a difference in the 1-s concentration levels, plume spread, and plume direction from panel to panel. Panel 4 shows the 30-min average concentration contours, where the inhomogeneity of the concentration field; after 30 min of release, is apparent. The highest concentration occurs near the downwind (NW) corner of the domain and surrounding the sources, where multiple sources contribute to the simulated concentrations. Even near the sources there are several zones of varying pheromone concentration and there are zones of lower concentration within zones of high concentration. These types of results can be coupled with information on the response levels of insects to help determine the most effective deployment pattern for artificial sources.

With this tool, the user can examine several scenarios and combine model output with expertise to determine the deployment pattern of the pheromone release devices. Questions similar to the following can be investigated with use of this modeling tool: What is the concentration of pheromone at 'X' distance from the semiochemical release(s); what is the minimum number of devices to deploy in order to blanket an area of 'X' hectares with a minimum concentration of 'Z'  $\mu\text{g/m}^3$  during the day; what type of deployment pattern works best; what is the concentration of pheromone along the perimeter of the area of concern; how might the deployment be configured to get a minimum concentration of 'Z'  $\mu\text{g/m}^3$  'Y' percentage of the time? The model can be applied to simulate a point source or multiple point sources, an area source (such as in pheromone flake deployment), and a line source (as in a swath deployment). As discussed in the previous section, the model has limitations under non-uniform canopy types and model performance has not been evaluated for distances greater than 30 m. The model is designed to be used as a tool to aid operational managers.

## 6. Conclusions

In general, the model successfully simulates maximum  $\chi/Q$  within a factor of two of the observations. Additionally, the sharp peaks and narrow widths common in the 1-s instantaneous data are simulated by the model; however, the simulated magnitude

may differ from the observed concentrations. This difference may be due to the simplistic nature of the model, which uses  $u$ ,  $v$ , and  $w$  wind components measured at the surrogate pheromone release location. Additional field studies with sonic anemometers placed at the outer edges of the experimental trial and used as input data in the model may prove to increase the capability of the model to simulate the magnitude of these peaks.

Future analysis of the model includes assessment of model performance under different canopy types and under one canopy type with varying stem densities. In future applications, we will work to incorporate the model features into a system that can employ less sophisticated meteorological data since high frequency, three-dimensional wind data are not available on a routine basis. This model could provide the basis for a web-based tool that can be used to guide synthetic pheromone deployment.

## Acknowledgements

The authors would like to especially recognize Dr. Patrick Shea for his expertise and help with this work. We thank Mike Huey, Wes Throop, Robert Beckley, Patricia Skyler, and Erik Lamb for their support in the field. Thank you to the AIRFIRE research team, PWFS, USDA FS for support. This research was supported and funded by the USDA Forest Service FHP/FHTET award No. 01-CA-11244225-025 and USDA Forest Service Projects FHTET TD.00.M03 and FHTET TD.00.M01.

## Appendix A

Simulated and observed  $\chi/Q$  [receptor concentration ( $\text{g m}^{-3}$ )/release rate ( $\text{g s}^{-1}$ )] arc maxima at 5, 10 and 30 m from the source for the lodgepole pine and ponderosa pine sites.

Arc maximum  $\chi/Q$  ( $\text{s m}^{-3}$ )

Date	Hour	5 m Observed	5 m Predicted	10 m Observed	10 m Predicted	30 m Observed	30 m Predicted
Lodgepole pine							
20 July 2000	11:30	0.081	0.135	0.027	0.053	0.003	0.008
20 July 2000	12:00	0.097	0.073	0.027	0.024	0.006	0.004
20 July 2000	12:30	0.092	0.057	0.021	0.019	0.010	0.003
20 July 2000	13:00	0.116	0.079	0.041	0.026	0.007	0.004
20 July 2000	13:30	0.201	0.093	0.047	0.029	0.009	0.004
20 July 2000	14:00	0.158	0.102	0.041	0.047	0.008	0.007
20 July 2000	14:30	0.123	0.096	0.036	0.033	0.006	0.005
20 July 2000	15:00	0.096	0.101	0.053	0.033	0.007	0.004
20 July 2000	15:30	0.126	0.099	0.040	0.036	0.012	0.005
21 July 2000	04:30	0.443	0.445	0.134	0.138	0.035	0.022
21 July 2000	05:00	0.835	1.132	0.319	0.422	0.017	0.078
21 July 2000	05:30	0.360	0.523	0.129	0.180	0.008	0.038
21 July 2000	06:00	0.219	0.267	0.114	0.127	0.010	0.025
21 July 2000	06:30	0.645	0.748	0.158	0.218	0.015	0.043
21 July 2000	07:00	0.574	0.794	0.237	0.251	0.092	0.044
21 July 2000	07:30	0.377	0.452	0.166	0.279	0.049	0.037
21 July 2000	08:00	0.481	0.410	0.282	0.215	0.057	0.046
21 July 2000	08:30	0.385	0.338	0.226	0.113	0.035	0.039
22 July 2000	04:30	0.217	0.305	0.063	0.127	0.013	0.033
22 July 2000	05:00	0.237	0.328	0.091	0.105	0.019	0.027
22 July 2000	05:30	0.226	0.570	0.125	0.193	0.012	0.035
22 July 2000	06:00	0.303	0.795	0.173	0.230	0.016	0.037
22 July 2000	06:30	0.437	0.584	0.094	0.187	0.033	0.020
22 July 2000	07:00	0.453	0.457	0.142	0.205	0.077	0.044
22 July 2000	07:30	0.293	0.379	0.137	0.135	0.037	0.038
22 July 2000	08:00	0.367	1.323	0.224	0.259	0.075	0.046
22 July 2000	08:30	0.488	0.473	0.080	0.350	0.027	0.054
23 July 2000	08:00	0.166	0.246	0.113	0.087	0.043	0.023
23 July 2000	08:30	0.209	0.267	0.061	0.135	0.046	0.022
23 July 2000	09:00	0.136	0.194	0.055	0.048	0.026	0.008
23 July 2000	09:30	0.215	0.150	0.077	0.070	0.028	0.009
23 July 2000	10:00	0.124	0.135	0.071	0.049	0.008	0.007
23 July 2000	10:30	0.070	0.083	0.021	0.032	0.005	0.004
23 July 2000	11:00	0.115	0.110	0.031	0.037	0.005	0.006
23 July 2000	11:30	0.085	0.071	0.030	0.025	0.005	0.004
23 July 2000	12:00	0.082	0.068	0.024	0.023	0.004	0.003
24 July 2000	06:30	0.136	0.150	0.123	0.082	0.021	0.015
24 July 2000	07:00	0.321	0.514	0.116	0.147	0.047	0.025
24 July 2000	07:30	0.594	0.490	0.351	0.662	0.111	0.121
24 July 2000	08:00	0.490	0.787	0.174	0.280	0.068	0.047
24 July 2000	08:30	0.205	0.504	0.123	0.155	0.026	0.021
24 July 2000	09:00	0.124	0.475	0.162	0.258	0.035	0.032
24 July 2000	09:30	0.136	0.176	0.083	0.068	0.016	0.009
24 July 2000	10:00	0.112	0.120	0.031	0.037	0.011	0.006
24 July 2000	10:30	0.084	0.096	0.040	0.032	0.008	0.005
25 July 2000	06:30	0.409	0.638	0.164	0.167	0.010	0.027
25 July 2000	07:00	0.670	1.463	0.369	0.365	0.064	0.048
25 July 2000	07:30	0.565	0.463	0.204	0.239	0.109	0.044
25 July 2000	08:00	0.618	1.300	0.245	0.420	0.078	0.088
25 July 2000	08:30	0.303	0.366	0.148	0.142	0.037	0.023
25 July 2000	09:00	0.276	0.385	0.151	0.181	0.034	0.024
25 July 2000	09:30	0.157	0.381	0.124	0.170	0.026	0.022
25 July 2000	10:00	0.324	0.310	0.128	0.101	0.034	0.014
25 July 2000	10:30	0.182	0.201	0.077	0.121	0.015	0.012

## Appendix A (Continued)

Arc maximum  $\chi/Q$  ( $\text{s m}^{-3}$ )

Date	Hour	5 m Observed	5 m Predicted	10 m Observed	10 m Predicted	30 m Observed	30 m Predicted
26 July 2000	06:30	0.536	0.672	0.133	0.224	0.028	0.028
26 July 2000	07:00	0.402	0.438	0.141	0.268	0.050	0.029
26 July 2000	07:30	0.526	0.468	0.228	0.239	0.035	0.031
26 July 2000	08:00	0.541	0.766	0.229	0.292	0.077	0.038
26 July 2000	08:30	0.264	0.210	0.126	0.079	0.034	0.028
26 July 2000	09:00	0.201	0.207	0.064	0.116	0.026	0.016
26 July 2000	09:30	0.155	0.305	0.095	0.119	0.018	0.014
26 July 2000	10:00	0.216	0.386	0.305	0.123	0.042	0.018
26 July 2000	10:30	0.153	0.209	0.244	0.112	0.022	0.013
27 July 2000	06:30	0.665	0.697	0.158	0.290	0.005	0.041
27 July 2000	07:00	0.661	0.758	0.275	0.284	0.013	0.034
27 July 2000	07:30	0.470	0.671	0.209	0.388	0.054	0.067
27 July 2000	08:00	0.628	0.694	0.236	0.258	0.064	0.035
27 July 2000	08:30	0.312	0.696	0.197	0.203	0.063	0.031
27 July 2000	09:00	0.383	0.155	0.139	0.170	0.036	0.032
27 July 2000	09:30	0.311	0.308	0.253	0.107	0.023	0.026
27 July 2000	10:00	0.752	1.393	0.515	0.361	0.075	0.064
27 July 2000	10:30	0.506	0.164	0.124	0.100	0.024	0.011
Ponderosa pine							
20 June 2001	14:30	0.054	0.042	0.022	0.015	0.003	0.003
20 June 2001	15:00	0.040	0.067	0.013	0.022	0.003	0.006
20 June 2001	15:30	0.052	0.039	0.012	0.018	0.003	0.005
20 June 2001	16:00	0.078	0.079	0.020	0.018	0.004	0.005
20 June 2001	16:30	0.105	0.042	0.009	0.017	0.003	0.003
21 June 2001	10:30	0.064	0.093	0.025	0.038	0.004	0.008
21 June 2001	11:00	0.138	0.121	0.047	0.042	0.003	0.008
21 June 2001	11:30	0.042	0.051	0.015	0.019	0.000	0.003
21 June 2001	12:00	0.065	0.036	0.017	0.014	0.000	0.004
21 June 2001	12:30	0.039	0.041	0.012	0.015	0.000	0.003
21 June 2001	13:00	0.058	0.055	0.012	0.019	0.003	0.004
21 June 2001	13:30	0.037	0.031	0.008	0.011	0.001	0.003
21 June 2001	14:00	0.058	0.072	0.009	0.022	0.000	0.004
21 June 2001	14:30	0.036	0.055	0.009	0.018	0.000	0.003
22 June 2001	09:30	0.061	0.126	0.022	0.035	0.003	0.006
22 June 2001	10:00	0.032	0.047	0.011	0.017	0.001	0.003
22 June 2001	10:30	0.031	0.055	0.012	0.016	0.001	0.004
22 June 2001	11:00	0.050	0.036	0.015	0.017	0.002	0.003
22 June 2001	11:30	0.045	0.061	0.015	0.020	0.001	0.004
22 June 2001	12:00	0.036	0.023	0.014	0.009	0.001	0.003
22 June 2001	12:30	0.033	0.055	0.008	0.017	0.000	0.003
22 June 2001	13:00	0.027	0.058	0.011	0.018	0.001	0.003
22 June 2001	13:30	0.036	0.052	0.011	0.016	0.001	0.003
23 June 2001	04:30	0.305	0.637	0.159	0.194	0.054	0.027
23 June 2001	05:00	0.277	0.426	0.126	0.136	0.037	0.025
23 June 2001	05:30	0.238	0.285	0.067	0.077	0.046	0.023
23 June 2001	06:00	0.192	0.224	0.069	0.056	0.026	0.010
23 June 2001	06:30	0.174	0.091	0.057	0.023	0.010	0.006
23 June 2001	07:00	0.248	0.434	0.125	0.128	0.008	0.021
23 June 2001	07:30	0.202	0.201	0.101	0.069	0.009	0.011
23 June 2001	08:00	0.156	0.155	0.052	0.049	0.002	0.008
23 June 2001	08:30	0.079	0.135	0.044	0.049	0.002	0.007
24 June 2001	04:30	0.145	0.225	0.050	0.064	0.008	0.020
24 June 2001	05:00	0.136	0.215	0.079	0.200	0.006	0.039
24 June 2001	05:30	0.147	0.187	0.084	0.080	0.027	0.015
24 June 2001	06:00	0.136	0.168	0.085	0.054	0.024	0.006
24 June 2001	06:30	0.108	0.220	0.041	0.060	0.011	0.013
24 June 2001	07:00	0.106	0.179	0.044	0.057	0.008	0.012
24 June 2001	07:30	0.094	0.200	0.035	0.063	0.006	0.009
24 June 2001	08:00	0.057	0.077	0.029	0.022	0.004	0.007
25 June 2001	14:30	0.050	0.080	0.014	0.032	0.002	0.009
25 June 2001	15:00	0.091	0.100	0.026	0.041	0.006	0.009
25 June 2001	15:30	0.094	0.175	0.024	0.050	0.003	0.013
25 June 2001	16:00	0.082	0.084	0.027	0.032	0.003	0.005
26 June 2001	08:30	0.158	0.215	0.036	0.064	0.004	0.012
26 June 2001	09:00	0.099	0.150	0.038	0.058	0.003	0.017
26 June 2001	09:30	0.112	0.219	0.023	0.075	0.004	0.013
26 June 2001	10:00	0.087	0.086	0.027	0.028	0.002	0.007
26 June 2001	10:30	0.115	0.066	0.028	0.025	0.001	0.006
26 June 2001	11:00	0.059	0.103	0.022	0.036	0.003	0.006
27 June 2001	08:00	0.182	0.043	0.056	0.018	0.011	0.006
27 June 2001	09:00	0.197	0.133	0.050	0.059	0.010	0.011
27 June 2001	09:30	0.185	0.175	0.054	0.055	0.013	0.009
27 June 2001	10:00	0.164	0.254	0.043	0.085	0.007	0.014
27 June 2001	10:30	0.064	0.094	0.018	0.041	0.002	0.008

## References

- Aukema, B.H., Clayton, M.K., Raffa, K.F., 2005. Modeling flight activity and population dynamics of the pine engraver, *Ips pini*, in the Great Lakes region: effects of weather and predators over short time scales. *Popul. Ecol.* 47, 61–69.
- Aylor, D.E., 1976. Estimating peak concentrations of pheromones in the forest. In: Anderson, J.F., Kaya, H.K. (Eds.), *Perspectives in Forest Entomology*. Academic Press, New York, NY, USA, pp. 177–188.
- Benner, R.L., Lamb, B., 1985. A fast response continuous analyzer for halogenated atmospheric tracers. *J. Atmos. Ocean. Technol.* 2, 582–589.
- Borden, J.H., 1995. From identifying semiochemicals to developing a suppression tactic: a historical review. In: Salom, S.M., Hobson, K.R. (Eds.), *Application of Semiochemicals for Management of Bark Beetle Infestations—Proceedings of an Informal Conference*. USDA For. Serv. Gen. Tech. Rep. INT-GTR-318. Ogden, UT, USA, pp. 3–10.
- Boylan, J.W., Russell, A.G., 2006. PM and light extinction model performance metrics, goals, and criteria for three-dimensional air quality models. *Atmos. Environ.* 40, 4946–4959.
- Brücher, W., Kerschgens, M.J., Martens, R., Thielen, H., Maßmeyer, K., 1998. Tracer experiments in the Freiburg-Schauenland area—comparison with flow and dispersion models. *Meteorol. Z.*, N. F. 7, 32–35.
- Davakis, E., Bartzis, J.G., Nychas, S.G., 2000. Validation of DIPCOT-II model based on Kincaid experiment. *Int. J. Environ. Pollut.* 14, 131–142.
- Davakis, E., Andronopoulos, S., Vlachogiannis, D., Venetsanos, A., Bartzis, J.G., Nychas, S.G., 2001. Validation of the Demokritos dispersion modelling system based on the Indianapolis experiment. *Int. J. Environ. Pollut.* 16, 88–100.
- Dinar, N., Kaplan, H., Kleiman, M., 1988. Characterization of concentration fluctuations of a surface plume in a neutral boundary layer. *Bound.-Lay. Meteorol.* 45, 157–175.
- Elkinton, J.S., Cardé, R.T., Mason, C.J., 1984. Evaluation of time-average dispersion models for estimating pheromone concentration in a deciduous forest. *J. Chem. Ecol.* 10, 1081–1108.
- Erbilgin, N., Nordheim, E.V., Aukema, B.H., Raffa, K.F., 2002. Population dynamics of *Ips pini* and *Ips grandicollis* in red pine plantations in Wisconsin: within- and between-year associations with predators, competitors, and habitat quality. *Environ. Entomol.*, 31, 1043–1051.
- Färbert, P., Koch, U.T., Färbert, A., Staten, R.T., Cardé, R.T., 1997. Pheromone concentration measured with electroantennogram in cotton fields treated for mating disruption of *Pectinophora gossypiella* (Lepidoptera: Gelechiidae). *Environ. Entomol.* 26, 1105–1116.
- Fares, Y., Sharpe, P.J.H., Magnuson, C.E., 1980. Pheromone dispersion in forests. *J. Theor. Biol.* 84, 335–359.
- Farrell, J.A., Murlis, J., Long, X., Li, W., Cardé, R.T., 2002. Filament-based atmospheric dispersion model to achieve short time-scale structure of odor plumes. *Environ. Fluid Mech.* 2, 143–169.
- Finnigan, J., 2000. Turbulence in plant canopies. *Annu. Rev. Fluid Mech.* 32, 519–571.
- Furniss, R.L., Carolin, V.M., 1977. *Western Forest Insects*. USDA Forest Service Misc. Pub. 1339, Washington, D.C., USA, 654 pp.
- Gifford, F., 1959. Statistical properties of a fluctuating plume dispersion model. *Adv. Geophys.* 6, 117–137.
- Hanna, S.R., 1984. The exponential probability density function and concentration fluctuations in smoke plumes. *Bound.-Lay. Meteorol.* 29, 361–375.
- Hanna, S.R., 1986. Spectra of concentration fluctuations: the two time scales of a meandering plume. *Atmos. Environ.* 20, 1131–1137.
- Holsten, E.H., Webb, W., Shea, P.J., Werner, R.A., 2002. Release rates of methylcyclohexenone and verbenone from bubble cap and bead releasers under field conditions suitable for management of bark beetles in California, Oregon and Alaska. *USDA For. Serv. Res. Pap. PNW-RP-544*, 21 pp.
- Holsten, E.H., Shea, P.J., Borys, R.R., 2003. MCH released in a novel pheromone dispenser prevents spruce beetle, *Dendroctonus rufipennis* (Coleoptera: Scolytidae), attacks in south-central Alaska. *J. Econ. Entomol.* 96, 31–34.
- Holzinger, R., Lee, A., Paw, U.K.T., Goldstein, A.H., 2004. Observations of oxidation products above a forest imply biogenic emissions of very reactive compounds. *Atmos. Chem. Phys. Discuss.* 4, 5345–5365.
- Koch, U.T., Cardé, A.M., Cardé, R.T., 2002. Calibration of an EAG system to measure airborne concentration of pheromone formulated for mating disruption of the pink bollworm moth, *Pectinophora gossypiella* (Saunders) (Lep. Gelechiidae). *J. Appl. Entomol.* 126, 431–435.
- Krasnec, J.P., Demaray, D.E., Lamb, B., Benner, R., 1984. An automated sequential syringe sampler for atmospheric tracer studies. *J. Atmos. Ocean. Technol.* 1, 372–378.
- Lanier, G.N., 1979. Protection of elm groves by surrounding them with multilure-baited sticky traps. *Bull. Entomol. Soc. Am.* 25, 109–111.
- Lee, A., Goldstein, A.H., Keywood, M.D., Gao, S., Varutbangkul, V., Bahreini, R., Ng, N.L., Flagan, R.C., Seinfeld, J.H., 2006a. Gas-phase products and secondary aerosol yields from the ozonolysis of ten different terpenes. *J. Geophys. Res.* 111, D07302.
- Lee, A., Goldstein, A.H., Kroll, J.H., Ng, N.L., Varutbangkul, V., Flagan, R.C., Seinfeld, J.H., 2006b. Gas-phase products and secondary aerosol yields from the photooxidation of 16 different terpenes. *J. Geophys. Res.* 111, D17305.
- Lewis, D.M., Chatwin, P.C., 1995. The treatment of atmospheric dispersion data in the presence of noise and baseline drift. *Bound.-Lay. Meteorol.* 72, 53–85.
- Mafra-Neto, A., Cardé, R.T., 1994. Fine-scale structure of pheromone plumes modulates upwind orientation of flying moths. *Nature* 369, 142–144.
- Murlis, J., Jones, C.D., 1981. Fine-scale structure of odour plumes in relation to insect orientation to distant pheromone and other attractant sources. *Physiol. Entomol.* 6, 71–86.
- Murlis, J., Willis, M.A., Cardé, R.T., 2000. Spatial and temporal structures of pheromone plumes in fields and forests. *Physiol. Entomol.* 25, 211–222.
- Mylne, K.R., Davidson, M.J., Thomson, D.J., 1996. Concentration fluctuation measurements in tracer plumes using high and low frequency response detectors. *Bound.-Lay. Meteorol.* 79, 225–242.
- Peterson, H., Lamb, B., 1992. Comparison of results from a meandering-plume model with measured atmospheric tracer concentration fluctuations. *J. Appl. Meteorol.* 31, 553–564.
- Peterson, H., Lamb, B., 1995. An investigation of instantaneous diffusion and concentration fluctuations. *J. Appl. Meteorol.* 34, 2724–2746.
- Peterson, H., Lamb, B., Stock, D., 1990. Interpretation of measured tracer concentration fluctuations using a sinusoidal meandering plume model. *J. Appl. Meteorol.* 29, 1284–1299.
- Peterson, H., Mazzolini, D., O'Neill, S., Lamb, B., 1999. Instantaneous spread of plumes in the surface layer. *J. Appl. Meteorol.* 38, 343–352.
- Raty, L., Drumont, A., De Windt, N., Grégoire, J.-C., 1995. Mass trapping of the spruce bark beetle *Ips typographus* L.: traps or trap trees? *Forest Ecol. Manage.* 78, 191–205.
- Reynolds, A.M., 2000a. Representation of internal plume structure in Gifford's meandering plume model. *Atmos. Environ.* 34, 2539–2545.
- Reynolds, A.M., 2000b. On the application of a Lagrangian particle-puff model to elevated sources in surface layers with neutral stability. *J. Appl. Meteorol.* 39, 1218–1228.
- Ross, D.W., Daterman, G.E., 1997. Using pheromone-baited traps to control the amount and distribution of tree mortality during outbreaks of the Douglas-fir beetle. *Forest Sci.* 43, 65–70.
- Salom, S.M., McLean, J.A., 1991. Flight behavior of scolytid beetle in response to semiochemicals at different wind speeds. *J. Chem. Ecol.* 17, 647–661.
- Santos, J.M., Griffiths, R.F., Roberts, I.D., Reis Jr., N.C., 2005. A field experiment on turbulent concentration fluctuations of an atmospheric tracer gas in the vicinity of a complex-shaped building. *Atmos. Environ.* 39, 4999–5012.
- Seigneur, C., Pun, B., Pai, P., Louis, J.-F., Solomon, P., Emery, C., Morris, R., Zahniser, M., Worsnop, D., Koutrakis, P., White, W., Tombach, I., 2000. Guidance for the performance evaluation of three-dimensional air quality modeling systems for particulate matter and visibility. *J. Air Waste Manage.* 50, 588–599.
- Seybold, S.J., Vanderwel, D., 2003. Biosynthesis and endocrine regulation of pheromone production in the Coleoptera. In: Blomquist, G.J., Vogt, R.G. (Eds.), *Insect Pheromone Biochemistry and Molecular Biology—The Biosynthesis and Detection of Pheromones and Plant Volatiles*. Elsevier Academic Press, Amsterdam, The Netherlands, pp. 137–200.
- Seybold, S.J., Bohlmann, J., Raffa, K.F., 2000. Biosynthesis of coniferophagous bark beetle pheromones and conifer isoprenoids: evolutionary perspective and synthesis. *Can. Entomol.* 132, 697–753.
- Shea, P.J., McGregor, M.D., Daterman, G.E., 1992. Aerial application of verbenone reduces attack of lodgepole pine by mountain pine beetle. *Can. J. Forest Res.* 22, 436–441.
- Sykes, R.L., Gabruk, R.S., 1997. A second-order closure model for the effect of averaging time on turbulent plume dispersion. *J. Appl. Meteorol.* 36, 1038–1045.
- Tchesslavskaja, K.S., Thorpe, K.W., Brewster, C.C., Sharov, A.A., Leonard, D.S., Reardon, R.C., Mastro, V.C., Sellers, P., Roberts, E.A., 2005. Optimization of pheromone dosage for gypsy moth mating disruption. *Entomol. Exp. Appl.* 115, 355–361.
- Thistle, H.W., Peterson, H., Allwine, G., Lamb, B., Strand, T., Holsten, E.H., Shea, P.J., 2004. Surrogate pheromone plumes in three forest trunk spaces: composite statistics and case studies. *Forest Sci.* 50, 610–625.
- Thykyer-Nielsen, S., Mikkelsen, T., 1993. RIMPUFF, Users Guide, Version 33. Risø National Laboratory, Denmark (Report), 60 pp.
- Turchin, P., Thoeny, W.T., 1993. Quantifying dispersal of southern pine beetles with mark-recapture experiments and a diffusion model. *Ecol. Appl.* 3, 187–198.
- US EPA, 2007. Guidance on the use of models and other analyses for demonstrating attainment of air quality goals for ozone, PM<sub>2.5</sub>, and regional haze. Publication No. EPA-454/B-07-002. EPA, April 2007, 253 pp.
- Venkatram, A., Brode, R., Cimarelli, A., Lee, R., Paine, R., Perry, S., Peters, W., Weil, J., Wilson, R., 2001. A complex terrain dispersion model for regulatory applications. *Atmos. Environ.* 35, 4211–4221.
- Vickers, N.J., Baker, T.C., 1992. Male *Heliothis virescens* maintain upwind flight in response to experimentally pulsed filaments of their sex pheromone (Lepidoptera: Noctuidae). *J. Insect Behav.* 5, 669–687.
- Vité, J.P., Gara, R.I., Von Scheller, H.D., 1964. Field observations on the response to attractants of bark beetles infesting southern pines. *Contrib. Boyce Thompson Inst.* 22, 461–470.
- Wilks, D.S., 2006. *Statistical Methods in the Atmospheric Sciences*. Academic Press, Burlington, MA, USA, 627 pp.
- Yee, E., Wilson, D.J., 2000. A comparison of the detailed structure in dispersing tracer plumes measured in grid-generated turbulence with a meandering plume model incorporating internal fluctuations. *Bound.-Lay. Meteorol.* 94, 253–296.